# Methodology for Studying Physical and Chemical Properties of the Air/Water Interface by Observing Excitation and Emission Spectra of Adsorbed Soluble Molecules with a Confocal Fluorescence Microscope

楊, 海涯

https://doi.org/10.15017/1654924

出版情報：九州大学, 2015, 博士（工学）, 課程博士
バージョン：

# Methodology for Studying Physical and Chemical Properties of the Air/Water Interface by Observing Excitation and Emission Spectra of Adsorbed Soluble Molecules with a Confocal Fluorescence Microscope

**Haiya YANG**

**Department of Molecular and Material Sciences,**
**Interdisciplinary Graduate School of Engineering Sciences,**
**Kyushu University**
**January, 2016**

# Table of Contents

# Abstract

The air/water interface is a universal but unique region. It is of great importance to understanding the air/water interface in physical, analytical, and environmental chemistry. Some physical and chemical properties of the air/water interface, like the pH at the air/water interface, are still controversial. Unlike commonly used surface-selective analytical methods including second-harmonic generation, sum-frequency generation and two-photon ionization, the sensitivity of a confocal fluorescence microscope (CFM) is so high that it enables us to observe the fluorescence emission of water-soluble fluorescent dyes adsorbed at the air/water interface even under the surface density of solute molecules being 1-$10^3$ molecule/$\mu m^2$. However, when it comes to broader and deeper application of studying physical and chemical properties of the air/water interface, there are still large rooms to completely improve the CFM equipment and to modify experimental procedures including theoretical and analytical developments.

In this dissertation, methodology is described for studying physical and chemical properties of the air/water surface by observing excitation and emission spectra of adsorbed soluble molecules with CFMs: a renovated-CFM calibrated and a semi-confocal fluorescence microscope (ScFM). Five chapters are successively developed to contribute to the methodology for understanding physical and chemical properties of the air/water interface, revolving with three central objectives: 1), to develop a CFM equipment in order to obtain a complete and corrected fluorescence spectra of soluble molecules at the air/water interface; 2), to develop a new method for determining pH at the air/water interface; and 3), to develop a ScFM as a new type of CFM for utilizing wavelength-tunable excitation in an UV region and for observing excitation spectra of soluble molecules adsorbed at the air/water interface. All conclusions in these chapters will significantly contribute to understanding the physical and chemical properties of the air/water interface.

In Chapter 1, backgrounds and objectives are described. Basic knowledge closely correlated was reviewed, including surface chemistry, the air/water interface, spectroscopic methods, tunable lasers, and fluorescence methods. Regarding studying physical and chemical properties of the air/water interface, and analytical methods for studying the air/water interface, research works are summarized, classified, and evaluated. For the CFM and fluorescent probes, fundamental knowledge as well as common research work are reviewed. Based on research works from predecessors, three original, essential and complicated research objectives are proposed.

In Chapter 2, development of a calibrated CFM equipment is described. A complete and corrected fluorescence spectrum of a fluorescent dye (rhodamine B, RhB) adsorbed at the

air/water interface is first obtained with the CFM developed. The experimental procedure to acquire such a fluorescence spectrum at the air/water interface is introduced. An updated alignment way proposed; a number of basic parameters for calibration obtained, including the time dependency of fluorescence intensity; the solution concentration dependence of fluorescence intensity; the depth resolution for the CFM; and the optimal data processing, which helps us to know the instrument of the CFM more and better.

In Chapter 3, a highly sensitive method for estimating pH at the air/water interface based on two pH-dependent dyes and the CFM is innovatively proposed. A relationship between the pH at the air/water interface and that in bulk solution is formulated in connection with the adsorption equilibrium and dissociation equilibrium of the dye adsorbed. Two ways for determining the unknown property $pK_{a,surf}$ of RhB molecules at the air/water interface are pointed out. The adsorption properties, the maximum surface density, and the adsorption equilibrium constants are estimated for both cationic and zwitterionic forms of RhB molecules at the air/water interface, with surface-tension measurements. As the basic fluorescence pH indicator, 5-(and-6)-carboxyseminaphthorhodafluor-1 is tried to be applied with this method, and some preliminary results are obtained. Owing to high sensitivity of this new method, this work provides new insight and inspiration for studying the water surface's acidity.

In Chapter 4, in order to observe fluorescence excitation spectra of soluble molecules adsorbed at the air/water interface, especially for aromatic hydrocarbons having no visible light-absorption, a ScFM is originally designed and constructed based on a total internal reflection illumination of tunable monochromatic UV light from a xenon lamp and a CFM. The theoretical feasibility to obtain fluorescence spectrum of soluble molecules adsorbed at the air/water interface surface-selectively with this microscope is confirmed. The fluorescence spectra of pyrene molecules are observed with this microscope. It is found that pyrene has a weak surface activity for observing fluorescence surface-selectively with the developed ScFM.

In Chapter 5, common conclusions for this dissertation are summarized, with future prospects proposed.

**Keywords:** the air/water interface, pH, confocal fluorescence microscope, rhodamine B, zwitterionic, semi-confocal fluorescence microscope, fluorescence spectrum, correction factors, excitation spectrum, pyrene.

# List of Symbols and Abbreviations

| | |
|---|---|
| BODIPY | boron-dipyrromethene |
| C | bulk concentration |
| CFM | confocal fluorescence microscope |
| $C(\lambda)$ | corrected fluorescence spectrum of RhB adsorbed at the air/water interface |
| d | solution density |
| $d_z$ | the solution thickness instead of the height of the probe volume |
| F | the value of force at this point displayed in this surface pressure |
| FWHM | full width at half maximum |
| h | the depth of glass plate immersing in solution |
| HD-SFG | heterodyne-detected electronic sum frequency generation spectroscopy |
| i | a component of $RhBH^+$ or $RhB^{\pm}$ |
| $I_E$ | the excitation laser power |
| $I(\lambda)$ | the emission spectrum of standard light source measured with the CFM |
| $K_a$ | the dissociation constant of RhB in the water bulk |
| $K_{ad}$ | the adsorption equilibrium constant |
| $K_{a,surf}$ | the dissociation constant of RhB at the air/water interface |
| $L(\lambda)$ | the ideal emission spectrum of standard light source |
| MD | molecular dynamics |
| $M(\lambda)$ | the measured fluorescence spectrum of RhB at the air/water interface |
| N | surface density |
| $N_{max}$ | the maximun surface density |

| | |
|---|---|
| PAHs | poly-aromatic cyclic hydrocarbons |
| pKa | the acid-base equilibrium constant |
| R6G | rhodamine 6G |
| $R_{f,i}$ | the ratio of fluorescent intensity detected for the surface |
| RhB | rhodamine B |
| $RhB^{\pm}$ | the zwitterionic form |
| $RhBH^{+}$ | the cationic form |
| S | the basal area of the glass plate |
| ScFM | semi-confocal fluorescence microscope |
| SFG | sum-frequency generation |
| SHG | second-harmonic generation |
| SNARF | 5-(and-6)-carboxyseminaphthorhodafluor-1 |
| TPI | two-photo ionization |
| $\alpha$ | the fraction of the acid form in the solution's surface region |
| $\gamma$ | surface tension |
| $\gamma(\lambda)$ | the correction factors of the fixed channel of the spectrometer in the CFM |
| $\eta$ | the efficiencies of fluorescence excitation detection per fluorescent molecule |
| $\eta_D$ | the proportionality constant for the equipment |
| $\nu$ | the fluorescence photo frequency |
| $\omega$ | the radius of probe volume confined in an cylindrical shape in the CFM |

# CHAPTER 1 Introduction

## 1.1 Background

Surface chemistry is one important subject of physical chemistry. In this subject, chemical processes and their precursor processes reacting in this interface are often discussed on the atomic or molecular scale. The interface is often considered as a transitional region of two different and closely contacted phases. It can be generally classified into gas-liquid interface, gas-solid interface, liquid-liquid interface, solid-solid interface, and so on.[1]

As shown in Fig. 1-1[2], surface chemistry has more than 200 years history since researchers initially started this subject. The first topics in the 1800s are catalysis, electrochemistry, photography and tribology, and they were all studied on the macroscopic scale. When it comes to the 2000s, some new topics, including surface change and electron transport, microporous solids, monolayer sciences, surface magnetic properties, surface mechanical properties, optical surfaces, polymer and bio-polymer surfaces and nanoparticle science, are

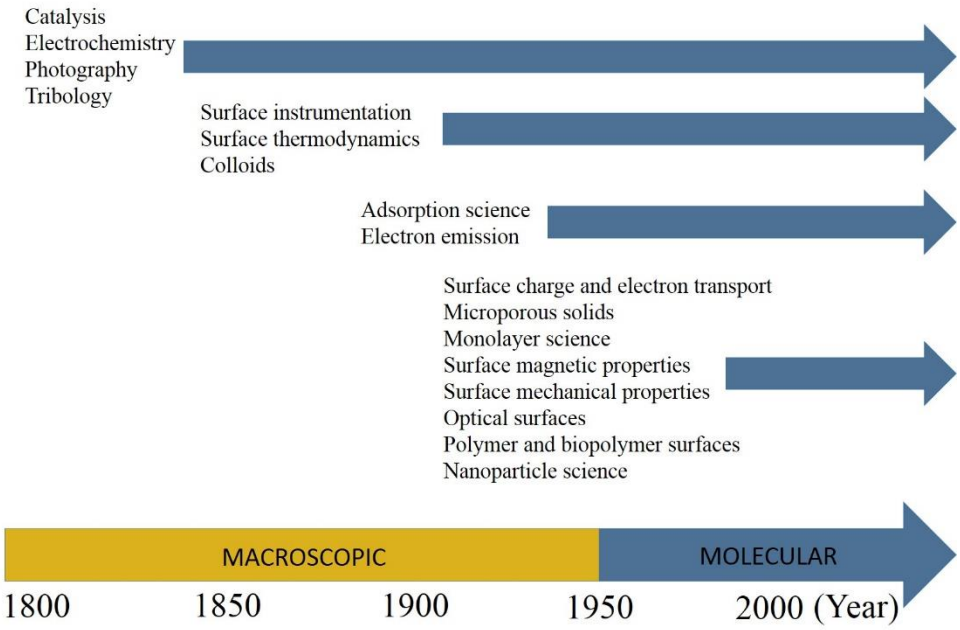


Fig. 1-1 Timeline of the historical development of surface chemistry

pouring out. On a whole, surface chemistry has been gradually developing from the macroscopic scale into the molecular scale in the past 200 years.

The basic thermodynamics of interfaces is discussed in Fig. 1-2[3]. Suppose there is a system with an interface consisting of three parts, phase $V^{\alpha}$, phase $V^{\beta}$, and the interface $\sigma$. Two conventions are often used to describe the basic thermodynamics of interfaces. One is the Gibbs convention, in which the interface $\sigma$ is considered to be a straight line. This is because the thickness of the interface is extremely small, particularly when in contrast to those of the other two different phases $V^{\alpha}$ and $V^{\beta}$. The other is the Guggenheim convention. The interface $\sigma$ is regarded as a transitional region between two different phases in this convention. Due to its practicality, the Gibbs convention is much more often to be accepted as the basic thermodynamics of interfaces.

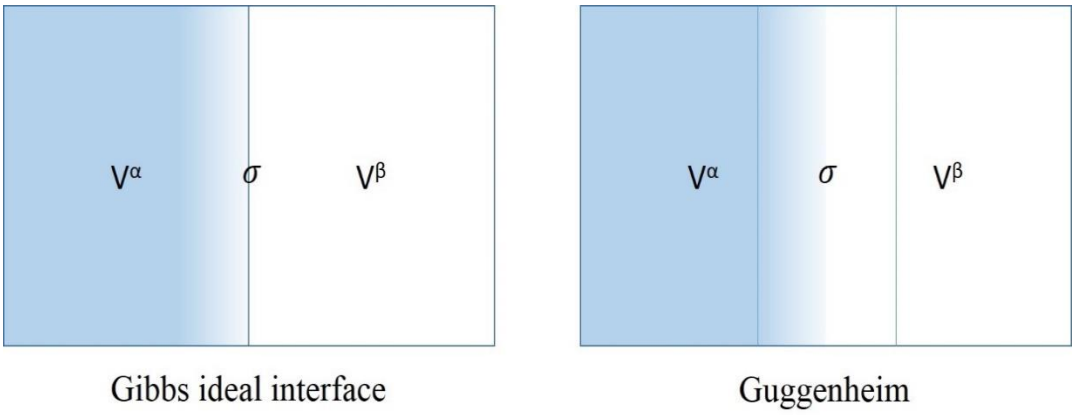


Fig. 1-2 The Gibbs convention and the Guggenheim convention of the basic thermodynamic of interfaces

The air/water interface is one of the most important branch of surface chemistry. About 71% of our earth is occupied with sea. The contacting region between the air and the sea is actually one biggest example of the air/water interface. Moreover, it is also easy for us to encounter some other examples of the air/water interface during our daily life, such as lakes, rivers, and

even beverages that exposed to the open air.

In contrast to the water bulk, there are mainly three particular properties for the air/water interface: 1) an extremely small thickness. It is revealed that the thickness of the air/water interface is less than 1 nm through molecular dynamics simulations[4] and vibrational sum-frequency generation experiments[5]; 2) high fluidity. Convection between the air phase and the water phase makes this interface flowable and unstable; 3) unique physical properties. The air/water interface has distinguished physical properties from that of the water bulk.

Given that the air/water interface is such a universal and unique region, and that understanding the air/water interface has great importance in physical, analytical, and environmental chemistry, study of the air/water interface has become a hot research topic in recent years.

As a common analytical method, spectroscopy has been frequently applied as a primary tool of chemical analysis in the past decades. It can be basically classified into three different kinds of analytical methods, including adsorption, emission and scattering of electromagnetic radiation by atoms or molecules. Researchers often study physical properties of atoms and molecules, or physical properties of their environment, like some atoms and molecules in the gas, liquid or solid phase, based on changes of their optical properties after absorbing electromagnetic radiation. Since quantum mechanics is closely interrelated to the spectroscopy, researchers often combine these two analytical methods to arrive at more comprehensive and accurate results.[6]

As known to all, a typical spectroscopic method has an instrumentation made up of a light source, monochromators, a specimen cell, a spectrometer, and so on. Laser is an innovative and high-priced light source with remarkable properties, such as directionality, monochromaticity, brightness and coherence. Some traditional lasers are introduced as follows: the ruby and alexandrite lasers, the titanium-sapphire laser, the neodymium-doped yttrium aluminum garnet laser, the diode or semiconductor laser, the helium-neon laser, the

argon ion and krypton ion lasers, the nitrogen laser, the excimer and exciplex lasers, the carbon dioxide laser, the dye lasers and laser materials in general.[6]

Since 1960, the invention of laser has surprisingly stimulated the development of spectroscopic methods. A variety of novel spectroscopic methods had been devised with laser sources, such as hyper Raman spectroscopy, stimulated Raman spectroscopy, coherent anti-Stokes Raman scattering spectroscopy, laser Stark spectroscopy, two-photo and multi-photon absorption, multiphoton dissociation and laser separation of isotopes, single vibronic level fluorescence, light detection and ranging, cavity ring-down spectroscopy, femtosecond spectroscopy and spectroscopy of molecules in supersonic jets.[6]

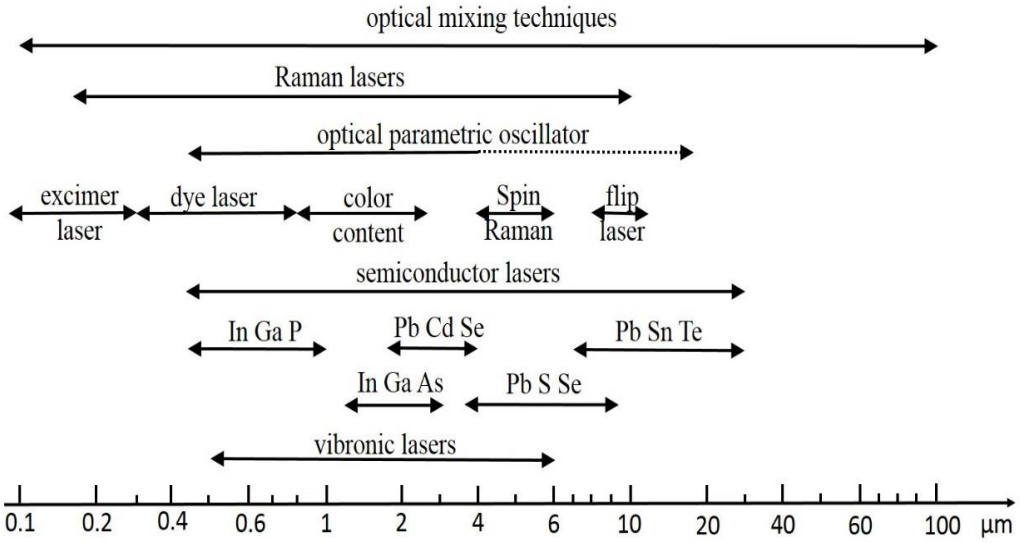


Fig. 1-3 Spectral ranges of different tunable coherent sources

Among all types of lasers in the developing history of lasers, tunable lasers are one superior type of laser with high attractiveness. Some common tunable coherent laser sources with their respective spectral ranges are listed in Fig. 1-3[7]. The most familiar ones for researchers may include the semiconductor-diode lasers, the tunable solid-state lasers, the color-center lasers, the dye lasers, the excimer lasers, and the free-electron lasers. Thanks to continuous

and widespread spectral ranges, these tunable lasers have been broadly applied into scientific research, despite of high prices.

Fluorescence microscopy is one spectroscopic method based on the emission of electromagnetic radiation by molecules or atoms. It has been extensively applied in the area of biological sciences in the past 30 years. In biochemistry and biophysics, fluorescence spectroscopy and time-resolved fluorescence are regularly regarded as main tools for scientific research. In biotechnology, flow cytometry, medical diagnostics, DNA sequencing, and genetic analysis, fluorescence microscopy is a widely used methodology. The greatest strength for fluorescence microscopy is high sensitivity. And for fluorescence spectroscopy, it is often required to correct emission spectra by means of comparing with known emission spectra of a standard compound, or correcting with a standard lamp, and correction factors using a quantum counter and scatter.[8]

As mentioned above, some fundamental knowledge closely correlated to this dissertation are briefly introduced. They are about the surface chemistry, the interface, the air/water interface, the spectroscopic methods, the tunable lasers, and the fluorescence microscopy.

## 1.2 State of the Art: Studying Physical and Chemical Properties of the Air/Water Interface

Owing to unique physical and chemical properties of the air/water interface, it is considerably meaningful to study them, especially when it comes to physical, analytical, and environmental chemistry.[9] Two ways of studying the air/water interface are habitually employed in reported work. One is to straightly study the air/water interface, like structures of water at the air/water interface. The other is to by the aid of the behavior of soluble molecules adsorbed at the air/water interface.

Hydrogen bonding and structure of water and adsorbates, as well as orientation of water molecules, are common research topics of studying the air/water interface. The aim is often about clarifying difference of structures of water molecules between the air/water interface and the bulk, and elucidating how water molecules at the air/water interface orientates differently from those in the bulk.

In the middle of all of the research topics of studying the air/water interface, one common type of research work is to study hydrogen bonding and structure of surface water, for a clearer understanding of surface and interfacial water structure and a deeper understanding of the behavior of water at its own surface. These research work also aims at elucidating interfacial water restructuring due to ions in order to develop a quantitative and predictive model for the effect of ions on the aqueous interface.[10-11] Some concrete examples are introduced through the following research findings.

P. A. Pieniazek *et al*.[12] claims no evidence was found of any special ice-like ordering at the surface of liquid water by using vibrational sum-frequency spectroscopy and theoretical analysis. I. V. Stiopkin *et al*.[13] studied free OD transition in the topmost water layer with isotopic dilution spectroscopy. By using deuterated water and isotopic dilution to reveal the vibrational coupling mechanism, they found that the free OD stretch is affected only by intramolecular coupling to the stretching of the other OD group on the same molecule. Z.

Zhang *et al*.[14] revealed interfacial water structure by using ultrafast two-dimensional surface vibrational spectroscopy. They made a conclusion that the structure of heavy water at the air/water interface displays short-lived heterogeneity and is very different from that at the water-lipid interface. C-S. Hsieh *et al*.[15] studied ultrafast reorientation of dangling OH groups at the air/water interface using femtosecond vibrational spectroscopy. The ultrafast reorientational motion of water molecules at the air/water interface were measured real-timely. It was found that the air/water interface is characterized by a population of dangling OH groups that rotates dramatically faster than bulk. N. Ji *et al*.[16] studied characterization of vibrational resonances at the air/water interface by phase-sensitive sum-frequency spectroscopy. They concluded that hydrated ions appearing at the interface may not disturb significantly the molecular bonding structure in the topmost surface later, but the surface filed they create could partially reorient molecules in the subphase.

Besides studying the air/water interface in a direct way, another mode of studying the air/water interface is by means of observing behavior changes of soluble molecules adsorbed at the air/water interface. These behavior changes may enable researchers to assess physical and chemical properties of the air/water interface.

One good example is ion solvation and isomerization reactions at the air/water interface. T.-M. Chang *et al*.[17] reported the recent advances in molecular simulations of ion solvation at liquid interface. They found that small ions are repelled from the liquid/vapor interface, which is consistent with the Gibbs adsorption equation. I. Benjanmin[18] reviewed the microscopic insight into solvation and reactions at liquid interface in recent years. He discussed isomerization reactions, solvation, ion transfer, and electron-transfer reactions, and presented unifying concepts for describing solvation and reactions at the liquid interfaces (liquid/vapor, liquid/liquid, and liquid/solid). In discussing measurement of bromide ion affinities for the air/water and dodecanol/water interfaces at molar concentrations by UV second harmonic generation spectroscopy, R. M. Onorato *et al*.[19] concluded that the structure of a liquid interface takes effects on the observed second harmonic generation

response of adsorbed anions, which is contributed to the number of ions at the interface and their effective hyperpolarizability.

Small molecules are also over and over again used as adsorbates to study their adsorptive behaviors at the air/water interface. These small molecules are including small carboxylic acids[20], polycyclic aromatic hydrocarbons (PAHs)[21], rhodamine 6G[22], methyl chloride and methyl alcohol[23], and so on. To be specific, by studying the protonation state of small carboxylic acids at the air/water interface, it is plausible to obtain the degree of acid dissociation at the air/water interface. The transport and photochemical transformation characteristics of PAHs at the air/water interface were studied, because PAHs are everywhere in the atmosphere and anthropogenic to human beings. PAHs strongly absorbs UV light between 300 nm and 420 nm and undergoes numerous photochemical reactions. By studying rhodamine 6G adsorbed at the air/water interface, it was first directly observed that the visible-IR sum frequency generation process in the electronically excited state of a model molecular system. This provides an effective probe for the electronically excited states of molecules at the molecular interface, as well as in the ordered molecular systems. Studying surface residence and uptake of gas-phase methyl chloride and methyl alcohol provides consequences for atmospheric chemistry, in particular for photodissociation of methyl chloride and methyl bromide when adsorbed on an aerosol surface.

Study of adsorptive behaviors of monolayers adsorbed at the air/water interface is another hot topic. I. I. Rzeźlnicka *et al*.[24] studied duramycin-induced destabilization of a phosphatidylethanolamine monolayer at the air/water interface with fluorescence microscopy and vibrational sum-frequency generation spectroscopy. While duramycin has no effect on the phosphatidylcholines lipid monolayers, it induces significant disorder of ethanolamine phospholipids molecules and causes an increase of the ethanolamine phospholipids monolayer surface pressure. Through a study of water penetration/accommodation and phase behavior of the neutral Langmuir monolayer, Z. Zhang *et al*.[25] confirmed the existence of an oriented water cluster species which has penetrated or accommodated into Langmuir

monolayer of the 8CB and 5CB molecules.

There are also research work focusing on adsorptive behaviors of surfactants adsorbed at the air/water interface. Y. You *et al*.[26] studied self-assembly of quaternary ammonium gemini surfactants at the air/water interface. The results reveal that the self-assembly of $C_{12}$-*s*-$C_{12}$ 2Br at the air/water interface is strongly promoted by the addition of sodium bromide. By studying interaction between anionic and cationic gemini surfactants at the air/water interface, J. Zhao *et al*.[27] reported that the surface tension $\gamma$ drops faster with total surfactant concentration.

Nanoparticles are also studied as adsorbates at the air/water interface. A single monolayer film was formed by spreading alkanethiol passivated silver nanoparticles at the air/water interface. This work revealed two process of the dynamics of the films at the air/water interface.[28]

As for biomacromolecules, H. Zheng *et al*.[29] studied protein-directed spatial rearrangement of glycolipids at the air/water interface, and found that lateral rearrangement of lipids on the surfaces of cell membranes takes an important effect in multivalent interactions. On the other hand, A. E. Miller *et al*.[30] studied the behavior of β-Amyloid 1-16 at varying pH at the air/water interface, and found that the β-Amyloid 1-16 peptide exhibits absorption and reorganization at the interface on very different time scales.

As presented above, we generally introduced the study of hydrogen bonding and structure of surface water, and the study of ion solvation and isomerization reactions, small molecules, monolayers, surfactants, nanoparticles and biomacromolecules adsorbed at the air/water interface. The corresponding research findings in recent years are also briefly reviewed. It is obvious that physical and chemical properties of the air/water interface distinguish from those of the water bulk, and that study of the air/water interface attracts a great deal of attention. Researchers used different kinds of analytical methods to study the air/water

interface and discovered many different kinds of new phenomena and mechanisms. Nevertheless, there are still a certain number of essential physical and chemical properties of the air/water interface that are still in controversy, like the pH. In other words, there are still many physical and chemical properties unknown for the air/water interface. So it is necessary to continue to study the air/water interface, in order to clarify other physical and chemical properties at the air/water interface.

## 1.3 State of the Art: Analytical Methods for Studying the Air/Water Interface

When it comes to studying the air/water interface, it is indispensable to use different analytical methods with their different strengths as main tools, according to different situations. The conventional analytical methods for studying the air/water interface are concisely introduced in the following text.

Molecular dynamics (MD) is a computer simulation method for studying the physical movements of atoms and molecules, and it is often applied in chemical physics, material science, and the modelling of biomolecules. By using numerical methods, MD simulation advantageously circumvents a thorny problem that some other analytical methods often confronts. As known to all, molecular systems typically consist of a large number of particles. So it is impossible to determine properties of certain complex systems in an experimental way. On the other hand, the limitations of MD has to be pointed out at the same time. Long MD simulations are mathematically ill-conditioned, generating cumulative errors in numerical integration that can be minimized with proper selection of algorithms and parameters, but not eliminated entirely.[31]

Molecular dynamics is used as a typical analytical method to study the air/water interface in a theoretical way, which becomes increasingly prevalent with the great development of computer sciences in recent years. Thanks to its avoiding unnecessary labor and time for experiments, researchers always combine it with other types of analytical methods together, in order to make a comprehensive analysis and a reliable conclusion. A. R. Miller *et al*.[30] investigated the behavior of β-amyloid 1-16 at the air-water interface at varying by the combination of second harmonic generation spectroscopy, Brewster angle microscopy, and MD simulations. In this research, they concluded that the β-amyloid 1-16 exhibits a large free energy of interfacial adsorption of -10.3 kcal/mol at both acidic and neutral bulk pH, but interestingly, it exhibits no presence at the air-water interface in a strongly basic solution.

Besides theoretical analysis, there also a variety of experimental methods for studying the air/water interface. However, it is uneasy to study the air/water interface in an experiment way. There are two primary difficulties that each mature analytical method has to overcome before being successfully applied into studying the air/water interface. One difficulty is to obtain fluorescence emissions at the air/water interface from the water bulk surface-selectively. Fluorescence emissions in the water bulk are often inclined to cause serious interference during analysis process. The other difficulty is that the sensitivity for one analytical method should be so high that optical signals at the air/water interface can be detected. This is because the surface density of molecules adsorbed at the air/water interface is less than 1 nanomole/$cm^2$. To date, the most conventional analytical methods for studying the air/water interface experimentally are sum-frequency generation (SFG), second-harmonic generation (SHG), and two-photon ionization.

Sum frequency generation is a nonlinear optical process, based on the annihilation of two input photons at angular frequencies $\omega_1$ and $\omega_2$. However, one photon at frequency $\omega_3$ is generated, simultaneously. The frequency $\omega_3$ is equal to the sum of the two input frequencies. Two conditions are essential for this kind of second order $\chi^{(2)}$phenomenon. One is that the light is interacting with matter, which is asymmetric (e.g., surfaces and interfaces). The other is that light has a very high intensity (typically from a pulsed laser).[32] Developed in 1987, this nonlinear laser spectroscopy method is often applied to analyze surfaces and interfaces. The advantages for SFG includes sensitivity in monolayer surface, operability in situ, and not causing much damage to the same surface.[33]

Some research work about studying the air/water interface with SFG are shown as follows. Y. R. Shen *et al*.[34] reviewed polar orientation of water molecules at interfaces with SFG. It was summarized that the spectrum of the SSP input/output polarization combinations usually shows an icelike peak at ~3200 $cm^{-1}$ and a liquid peak at ~3400 $cm^{-1}$, plus a narrow dangling OH peak at ~3700 $cm^{-1}$ if the interface is hydrophobic if the interface is hydrophobic. This result suggests interfacial water molecules form a partially disordered hydrogen-bonding

network. G. L. Richmond[11] reviewed molecular bonding and interactions at aqueous surfaces as probed by SFG. It includes hydrogen bonding and structure of water at the air/water interface, and adsorbate structure and boning at aqueous surfaces.

Heterodyne-detected electronic sum frequency generation spectroscopy (HD-SFG) is a newly presented technique derived from SFG.[35] It has high sensitivity allowing surface-selective measurements of vibrational spectra at submonolayer surface coverage, as low as a few percent of a monolayer. In conventional (homodyne-detected) SFG spectroscopy, the signal intensity decreases quadratically with decreasing surface coverage. However, when it comes to HD-SFG, the scaling is linear, and the signal is amplified by interference with a reference beam, which improves sensitivity and detection limits significantly.

Some new research work has already reported the merits of this new technique in its application. H. Watanabe *et al*.[36] tried to obtain a microscopic picture of interfacial solvation by using a close combination of heterodyne-detected electronic sum frequency generation spectroscopy, polarization second harmonic generation, and molecular dynamics simulation. A surface-active solvatochromic polyatomic molecule, coumarin 110 was spread at the air/water interface. S. Yamaguchi *et al*.[37] reported "up" versus "down" alignment of interfacial molecules with heterodyne-detected electronic sum frequency generation spectroscopy. HD-ESFG provides linear $\chi^{(2)}$ spectra that have unambiguous information on the "up" versus "down" alignment of interfacial molecules.

Two dimensional SFG is a novel advanced technique of SFG. With a novel instrumentation for pump-probe SFG setup and the first 2D-SFG experiment on a monolayer of dodecanol on water, it was expected that this instrumentation can be used to study the dynamics of water molecules at the neat air/water interface.[38] With this new technique, Z. Zhang *et al*.[39] revealed ultrafast vibrational energy transfer at the air/water interface. The occurrence of surprisingly fast intra- and intermolecular energy transfer processes at aqueous interfaces was revealed. It was shown that energy transfer among O-D stretching modes of water on the

surface is rapid and efficient and that O-D-excitations move both along the surface plane and down into the bulk. J. Bredenbeck *et al*.[40-41] discussed the implementation of ultrafast 2D-IR SFG spectroscopy. This is another new technique and can be applied into studying the structure and dynamics of interfacial water in various systems. The authors also presented a complete analytical theory of surface 2D-IR-SFG spectroscopy and demonstrated that heterodyne detection of the 2D SFG signals will further facilitate the interpretation of the experimental results in terms of interfacial vibrational coupling.

Second-harmonic generation is also a nonlinear optical effect, which is only allowed in mediums without inversion symmetry. It is a special case of SFG. In a nonlinear optical process for SHG, photons with the same frequency interacting with a nonlinear material are effectively "combined" to generate new photons with twice the energy, and therefore twice the frequency and have the wavelength of the initial photons.[42] With SHG and other spectroscopic methods, O. N. Slyadneva *et al*.[43] presented orientation and aggregation behavior of rhodamine dye with long alkyl chains at the air/water interface under compression using absorption and fluorescence spectroscopies and the SHG technique.

Laser two-photo ionization is another surface-selectively analytical method, based on a physical process in which an ion is formed from the interaction of a photon with an atom or molecule. The TPI is sometimes selected as an analytical method to study the air/water interface, because it may have higher sensitivity and a lower detection limit than SHG technique dose.[44] M. Sato *et al*.[45] proposed a new method to determine the equilibrium between the bulk and the surface by directly measuring surface concentrations using laser two-ionization. M. Sato *et al*.[46] also reported the surface density and polarization dependence of the TPI signal of the pyrenehexadecanoic acid monolayer at the air/water interface. They found that found a clear signal intensity dependence on excitation laser beam polarization, which should be related to the orientation of these molecules on the water surface.

As discussed above, we paraphrased several analytical methods for studying the air/water interface experimentally. However, these research work introduced above are all related to the study of the air/water interface. In fact, even when it comes to other interfaces, there are also many other kinds of analytical methods. J. M. Perera *et al*.[47] reviewed spectroscopic studies of molecular interaction at the liquid-liquid interface. It documents the scope of these approaches and summarizes a representative sample of the available data for several liquid-liquid interface. S. Tsukahara[48] dominantly summarized recent analytical methodologies on equilibrium, kinetics, and dynamics, at liquid/liquid interface with brief explanations. H. Nagatani *et al*.[49] focus on recent progress and applications of potential-modulation spectroeletrochemical methods at solid/liquid and liquid/liquid interfaces. The advantages of the use of potential-modulation methods are also highlighted. I. Benjamin[50] reviewed static and dynamic electronic spectroscopy at liquid interfaces (liquid/vapor and liquid/liquid interfaces), and concluded that the unique properties of the liquid interface region have a marked signature on the electronic absorption spectra and solvation dynamics of adsorbed dye molecules.

Although there are many, mature and accurate analytical methods that can be used to study the air/water interface, these analytical methods still have a common serious limitation. The sensitivity in each of these analytical methods is not high enough to be applied into studying extremely dilute solutions. Therefore, in order to eliminate probe effects existing in most analytical methods, it is expected to have another new analytical method with much higher sensitivity to study the air/water interface surface-selectively.

## 1.4 Confocal Fluorescence Microscope

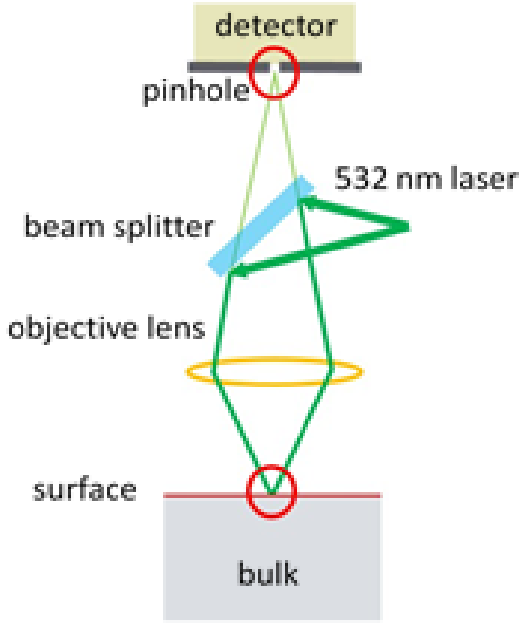


Fig. 1-4 A schematic setup of a confocal fluorescence microscope

Confocal microscopy is an optical imagining technique for increasing optical resolution and contrast of a micrograph. It was based on an objective lens to focus a laser exciting light and a small pinhole to eliminate out-of-focus fluorescence light generated at a specimen. This technique is extensively applied in the scientific and industrial communities and typical application in life sciences, semiconductor inspection and materials sciences.[51] A schematic setup of a typical confocal fluorescence microscope (CFM) is demonstrated in Fig. 1-4. A focus of a laser exciting light and a small detector pinhole are the two most essential factors for a CFM. The laser exciting light is focused on one point of a specimen through an objective lens, whereas fluorescence light generated at the specimen are collected by the objective lens, focused by another lens, and transmitted into a detector through a small pinhole. The out-of-focus fluorescence light is naturally rejected outside the small pinhole. For a confocal laser-scanning microscope, depth discrimination in the CFM also enables a view of z-axis, and thus the feasibility to capture 3D images of a specimen.[52]

There are also a great deal of research around the application of a CFM in recent years. By using a CFM coupled with a diffraction-limited laser beam and a high efficiency detection system, S. Nie *et al*.[53] studied the diffusive movement and emission process of individual fluorescent molecules in the liquid phase at room temperature. It was found that fluorescence-cycle saturation at the single-molecule level and multiple recrossings of a single molecule into and out of the probe volume as well as the triplet state. Y. Kitazumi *et al*.[54] successfully imaged the inhomogeneity at the 1,2-dichloroethane/water interface caused by the transfer of dodecyl sulfate across the interface using a CFM and a probe of a fluorescence phospholipid. J. W. Blunt[55] showed a work of a single molecule with atomic resolution under the microscope for elucidation of chemical structure.

Some research work related to the development of a CFM also spring up in the past decades. In order to increase the axial resolution of a confocal microscope, M. Schrader *et al*.[56] obtained the three-dimensional optical transfer functions of different types of 4pi microscopes from experimental data, and increased the axial resolution of a confocal microscope. V. Hischfeld *et al*.[57] developed a cryostat suitable for a laser scanning confocal microscope to investigate single molecules at liquid nitrogen with high sensitivity and accuracy. S. Selci *et al*.[58] reported design and implementation of a new reflectance laser scanning confocal system with spectroscopy imaging capabilities. This apparatus enables them to collect each single scanning point as a whole spectrum in a continuous range, associated with the optical section imaging possibilities typical of a confocal setup. B. S. Chun *et al*.[59] constructed a beam scanning chromatic confocal microscope using the galvanometric transverse scanning mechanism and investigated the effect of transverse point beam scanning in chromatic confocal microscopy.

In our research group, a CFM was developed to as an innovative tool to study the air/water interface. In the developing process, Y.-Q. Li *et al*.[60] first developed a fiber bundle confocal fluorescence microspectrometer that can be used to obtain a spectrum of individual fiber spots on the charge-coupled device. Afterwards, a new and simple approach to align this

CFM for spectroscopic measurements at the air/water interface was also proposed.[61] This approach is based on using a fiber bundle to collect optical signals to use satellite lines to the excitation laser as a reference light for alignment. This CFM was then tried to be used to obtain the fluorescence spectrum of a porphine at the air/water interface.[62] It was found that the unique spectral fluctuations of the phosphine at the air/water interface was attributed to cluster formation of the neutral porphine and an inhomogeneous distribution of solutes. X.-Y. Zheng *et al*.[63] also successfully observe fluorescent photon bursts from the insoluble RhC18 dye molecules by using a confocal fluorescence photon-counting microscopy. However, these target molecules are still considered to be as insoluble molecules at the air/water interface, because its solubility in water is extremely low.

It was before long to achieve the application of the CFM to soluble molecules adsorbed at the air/water interface. X.-Y. Zheng *et al*.[64] first reported that the CFM can also be used to study soluble molecules at the air/water interface with high surface-selectivity, by spreading at the air/water interface with a surface density of $10^{-16}$ mol/cm$^2$, and observing the temporal fluctuation of fluorescence photon bursts of R6G molecules at the air/water interface. Furthermore, the effects of acidity of the bulk solutions on the fluorescence properties and adsorption behavior of R6G molecules at the air/water interface were also investigated.[65] It is also concluded that CFM is also can to be used for interface-selective observations of dye molecules at oil-water interfaces.[66]

Laser-induced fluorescence microscopy is also one special technique of the fluorescence microscopy. Y.-Q. Li *et al*.[67] used a laser-induced fluorescence microscopy to study the fluorescence spectrum of an insoluble molecule of chromophore meso-α,β,γ,δ-tetraphenylporphine at the air/water interface. It was concluded that the air/water interface is hydrophobic and less polar than the water bulk. M. N. Slyadnev *et al*.[68] studied the properties and behavior of a rhodamine and a cyanine dye by using the laser-induced fluorescence microscopy. It was concluded that the spectrum on the water interface is similar to that in bulk nonpolar solvent. B. T. Mmereki *et al*.[69] studied pyrene at an organic coated air/water

interface with the laser- induced fluorescence spectroscopy. It was shown that partitioning of pyrene is enhance up to a factor of 2 at the air/water interface when the interface is coated with an organic film.

As described above, confocal fluorescence microscopy has been continuously developed and applied into studying the air/water interface. Thanks to its high sensitivity and surface-selectivity, a large number of new scientific findings at the air/water interface have been obtained with this new technique. However, there are still two obvious, vital and tough defects in the CFM that we have to point out: 1) a complete and correct fluorescence spectrum of soluble molecules adsorbed at the air/water interface has not yet been obtained; 2) the 532 nm laser in the CFM as the only exciting light critically limits species-selectivity and range of applications. Due to these two limitations, there are still a lot of essential work in the CFM that we should do.

## 1.5 Fluorescent Probes

Fluorescence probes is one of the most important areas of fluorescence spectroscopy. According to properties of fluorescence probes, researchers are able to understand physical and chemical properties of matters or their environments, based on information available from the experiments, such as wavelength and time resolution. Mostly, the molecules of interest are nonfluorescent or have faint fluorescence. Good example are DNA and lipids. They start to cause useful fluorescence when labeled with extrinsic probes. Proteins are often labeled with chromophores with longer excitation and emission wavelengths than the aromatic amino acids. Among thousands of fluorescent probes, they can be primarily divided into intrinsic probes and extrinsic probes. Intrinsic probes are those that occur naturally, whereas extrinsic probes are those that added to the sample to provide fluorescence when none exists, or to change the spectral properties of the sample.[8]

Only fluorescent probes that are sensitive to pH can be used to measure pH. This kind of fluorescent probes is regarded as fluorescence pH probes. As a research hotspot, monitoring pH changes inside living cells is essential for studying cellular internalization pathways, such as phagocytosis, endocytosis, and receptor ligand internalization. J. Han *et al*.[70] reviewed fluorescence indicators for intracellular pH and classified pH indicators to small fluorescent organic molecules, nanoparticles and fluorescent proteins. In the study of imaging intracellular pH in a reef coral and symbiotic anemone, A. A. Venn *et al*.[71] also determined intracellular pH by loading cells with pH sensitive fluorescent probe, carboxyseminaphthorhodafluor-1 (SNARF). SNARF is a ratiometric fluorescence pH probe that has dual emission wavelength at an emission of 585 nm and 640 nm.

Often, researchers developed different kinds of fluorescent pH probes for meeting their own specific requirements in experiments. These fluorescent pH probes of interest can be synthesized in many different ways. One common type is to develop fluorescent pH probes based on small organic molecules. N. Boens *et al*.[72] designed and synthesized a ratiometric fluorescent pH indicator based on boron-dipyrromethene (BODIPY, a class of fluorescent

dyes)[73] by conjugative linking the BODIPY fluorophore at the 3-position to the pH-sensitive ligand imidazole through an ethenyl bridge. This pH indicator can be used for measurements in the pH range of 5-7, under an exciting wavelength of 520 nm. It was demonstrated that it is feasible to rationally design a near-neutral fluorescent pH probe which has many desirable properties. S. Chen *et al*.[74] developed a small organic fluorogen with Aggregation-induced emission characteristics, TPE-Cy, for intracelluclar pH sensitive. This fluorescent probe is considered to be a full range intracellular pH, because the intensity ratio of dual emission peaks at 489 nm and 615 nm varies with the pH range of pH (4.7-8.0), under an exciting wavelength of 380 nm.

Another common type of developing fluorescence pH probes is based on nanoparticles. M. J. Marín *et al*.[75] reported a dual emissive pH probe based on the self-assembly of two fluorescent ligands, that includes a PET-based pH sensor, to the surface of gold nanoparticles. The two emission peaks at 580 nm and 421 nm varies with pH (3.7-8.1), under an exciting wavelength of 364 nm. For intracellular pH measurement, K. Zhou *et al*.[76] reported design of a series of pH-activatable micellar nanoparticles with tunable and ultrasensitive pH response in the physiological range between 5.0 and 7.4, based on the supramolecular self-assembly of ionized block copolymer micelles. K. Zhou *et al*.[77] also demonstrated a robust and general strategy to create a series of pH-tunable, multicolored fluorescence nanoparticle to investigate intracellular pH. The fluorescence wavelength range is between 500 and 820 nm, the multicolored, pH tunable fluorescent nanoplatfom. J. Lei *et al*.[78] presented a new type of ratiometric fluorescence pH sensor, this sensor is based on mesoporous silica nanoparticles and Förster resonance energy transfer. Good sensing capability was also found for hydrogen ions under a single-wavelength excitation.

Besides, S. Wu *et al*.[79] prepared mesoporous silica nanoparticles containing lysosome activable rhodamine-lactam for ratiometric sensing of lysosomal pH changes in living cells with high sensitivity by confocal microscopy or flow cytometry via single-wavelength excitation. In the development of sensor technology, H. Sun *et al*.[80] introduced a new

strategy to expand the pH measurement range by labelling nanoparticles with dual or multiple pH sensitive fluorophores. One example is labelling polyacrylamide nanoparticles with two pH sensitive fluorophores Oregon (pKa＝4.8) and fluorescein (pKa＝6.4), and the pH inert fluorophore RhB, the nanosensor is capable of measuring a pH range from 3.9 to 7.3. Another nanosensor is containing two pH sensitive fluorophores Oregon and BCECF and the pH inert fluorophore Alexa 633. And this nanosensor is capable of measuring a pH from 3.9-7.9.

For fluorescence pH probes based on carbon nanodots and polymer dots, there are also a little intriguing research work in the recent years**.** In order to measure intracellular of whole cells, W. Shi *et al*.[81] reported a tunable ratiometric fluorescent pH sensor based on dual-labeled carbon nanodots, with an exciting wavelength of 488 nm and dual emission peaks at 515 nm and 575 nm varying with pH (5-9) . Y.-H. Chan *et al*.[82] reported the design and performance of the first pH-sensitive polymer dots. Semiconducting polymer-based nanoparticles with a linear pH sensing range between 5 and 8 are suitable for most biological applications

It is also common to encounter fluorescence pH probes based on nanogels. H.-S. Peng.[83] presented for the first time a ratiometric fluorescent nanogel for sensing of intracellular pH. The intensity ratio of dual emission peaks are 500 nm and 620 nm varies with pH (4.92-9.18), under an exciting wavelength of 450 nm.

There are also fluorescence pH probes based on dentrimer and proteins. L. Albertazzi *et al*.[84] reported a dentrimer-based ratiometric pH sensor in living cells, which overcomes some severe limitations of organic dyes. In this sensor, the dentrimers act as scaffolds able to carry sensing fluorophers together with other analyte-insensitive dyes and therefore make it possible to perform ratiometric imaging. M. Tantama *et al*.[85] reported a fluorescence protein probe of pHRed that is excitation ratiometric with a pKa of 6.6. It has a fluorescence peak at 610 nm, and exhibits dual excitation peaks at 440 nm and 585 nm. The intensity ratio of these two excitation peaks varies with pH (5.5~9.0).

Among numerous florescent pH probes in all of the reported works, a proper fluorescent pH probe should be developed and selected carefully according to experimental requirements and experimental conditions. When it comes to our case of selecting a fluorescence pH probe to estimate pH at the air/water interface with the CFM, there are three requirements that we have to be meet: 1) fluorescent ratiometric probes; 2) exciting wavelength of 532 nm; 3) emission wavelength between 550 and 650 nm. Therefore, with the development of the instrumentation of the CFM, it is also crucial for us to screen for proper fluorescence probes to measure the pH at the air/water interface under this kind of experimental conditions.

## 1.6 Research Objectives

Above all, although research findings concerning the air/water interface, its physical and chemical properties, related analytical methods, CFM and fluoresce probes emerge in large numbers over the past few years, a certain number of critical defects do exist and have to be pointed out. 1) Some physical and chemical properties of the air/water interface, like the pH, are still ambiguous and needs to be further clarified, especially with a new analytical method that has much higher sensitivity to eliminate the probe effects; 2) A complete and correct fluorescence spectrum of soluble molecules adsorbed at the air/water interface has not yet been obtained; 3) The 532 nm laser in the CFM as the only exciting light source critically limits species-selectivity and range of applications.

Against these defects in the past research work with regard to the air/water interface, its physical and chemical properties, related analytical methods, CFM and fluoresce probes, there are still a lot of essential work that we should do. Therefore, with the purpose of pushing forward cogitation of the fields stressed above, three original and vital research objectives are proposed in this dissertation as follows:

1) To develop a CFM equipment in order to obtain a complete and corrected fluorescence spectra of soluble molecules at the air/water interface

2) To develop a new method for determining pH at the air/water interface

3) To develop a new type of CFM, semi-confocal fluorescence microscope, for utilizing wavelength-tunable excitation in an UV region and for observing excitation spectra of soluble molecules adsorbed at the air/water interface

## References


1. X. Fu, W. Shen, T. Yao, and W. Hou, *"Wuli Huaxue* (Physical Chemistry, in Chinese)", 5th ed., **2006**, Chap.13, Higher Education Press, Beijing.
2. G. A. Somorjai and Y. Li, *"Introduction to Surface Chemistry and Catalysis"*, 2nd ed., **2010**, Chap.1, John Wiley & Sons, Inc., New Jersey.
3. H. Butt, K. Graf, and M. Kappl, *"Physics and Chemistry of Interfaces",* **2006**, Chap.3, Wiley-VCH Verlag GmbH & Co. KGaA, Weinheim.
4. L. X. Dang and T.-M. Chang, *J. Chem. Phys*., **1997**, *106*, 149.
5. E. A. Raymond, T. L. Tarbuck, M. G. Brown, and G. L. Richmond, *J. Phys. Chem. B*, **2003**, *107*, 546
6. J. M. Hollas, *"Modern Spectroscopy"*, 4th ed., **2004**, Chap. 9, John Wiley & Sons Ltd, Chichester.
7. W. Demtröder, *"Laser Spectroscopy Vol. 1: Basic Principles"*, 4th ed., **2008**, Chap. 5, Springer-Verlag, Berlin Heidelberg.
8. J. R. Lakowicz, *"Principles of Fluorescence Spectroscopy"*, 3rd ed., **2006**, Chap. 1, Springer Science+Business Media, LLC, New York.
9. A. Harata, M. Sato, and T. Ishioka, *"Charged Particle and photo Interactions with Matter: Recent Advances, Applications, and Interfaces"*, ed. Y. Hatano, Y. Katsumura, and A. Mozumder, **2010**, CRC press, Boca Raton, 445.
10. S. Gopalakrishnan, D. Liu, and H. C. Allen, *Chem. Rev.,* **2006**, *106*, 1155.
11. G. L. Richmond, *Chem. Rev.,* **2002**, *102*, 2693.
12. P. A. Pieniazek, C. J. Tainter, and J. L. Skinner, *J. Am. Chem. Soc.,* **2011**, *133*, 10360.
13. I. V. Stiopkin, C. Weeraman, P. A. Pieniazek, F. Y. Shalhout, J. L. Skimmer, and A. V. Benderskii, *Nature*, **2011**, *474*, 192.
14. Z. Zhang, L. Piatkowski, H. J. Bakker, and M. Born, *J. Chem. Phys.,* **2011**, *135*, 021101.
15. C-S. Hsieh, R. K. Campen, A. C. V. Verde, P. Bolhuis, H-K. Nienhuys, and M. Bonn, *Phys. Rev. Lett.*, **2011**, *107*, 116102.
16. N. Ji, V. Ostroverkhov, C. S. Tian, and Y. R. Shen, *Phys. Rev. Lett.*, **2008**, *100*, 096102.
17. T.-M. Chang and L. X. Dang, *Chem. Rev.,* **2006**, *106*, 1305.

18. I. Benjamin, *Chem. Rev.*, **1996**, *96*, 1449.
19. R. M. Onorato, D. E. Otten, and R. J. Saykally, *J. Phys. Chem. C*, **2010**, *114*, 13746.
20. N. Ottosson, E. Wernersson, J. Söderström, W. Pokapanich, S. Kaufmann, S. Svensson, I. Persson, G. öhrwall, and O. Björneholm, *Phys. Chem. Chem. Phys.,* **2011**, *13*,12261.
21. J. Chen, F. S. Ehrenhauser, K. T. Valsaraj, and M. J. Wornat, *J. Phys. Chem. A*, **2006**, *110*, 9161.
22. D. Wu, G-H. D, Y. Guo, and H-F. Wang, *J. Phys. Chem. A.,* **2009**, *113*, 6058.
23. K. Harper, B. Minofar, M. R. Sierra-Hernandez, N. N. Casillas-Ituarte, M. Roeselova, and H. C. Allen, *J. Phys. Chem. A.,* **2009**, *113*, 2015.
24. I. I. Rzeźnicka, M. Sovago, E. H. G. Backus, M. Bonn, T. Yamada, T. Kobayashi, and M. Kawai, *Langmuir,* **2010**, *26(20)*, 16055.
25. Z. Zhang, D-S. Zheng, Y. Guo, and H-F. Wang, *Phys. Chem. Chem. Phys.,* **2009**, *11*, 991.
26. Y. You, J. Zhao, R. Jiang, and J. Cao, *Colloid. Polym. Sci.*, **2009**, *287*, 839.
27. J. Zhao, J. Liu, and R. Jiang, *Colloids Surf., A,* **2009**, *350*, 141.
28. G. Martin-Gassin, Y. E. Harfouch, E. Benichou, G. Bachelier, I. Russier-Antoine, C. Jonin, S. Roux, O. Tillement, and P.-F. Brevet, *J. Phys. Condens. Matter, A*, **2008**, *20*, 055228.
29. H. Zheng and X. Du, *J. Phys. Chem. B*, **2010**, *114*, 577.
30. A. E. Miller, P. B. Peterson, C. W. Hollars, and R. J. Saykally, *J. Phys. Chem. A,* **2011**, *115*, 5873.
31. https://en.wikipedia.org/wiki/Molecular_dynamics
32. https://en.wikipedia.org/wiki/Sum-frequency_generation
33. https://en.wikipedia.org/wiki/Sum_frequency_generation_spectroscopy
34. Y. R. Shen and V. Ostroverkhov, *Chem. Rev.*, **2006**, *106*, 1140.
35. I. V. Stiopkin, H. D. Jayathilake, A. N. Bordenyuk, and A. V. Benderskii, *J. Am. Chem. Soc.,* **2008**, *130*, 2271.
36. H. Watanabe, S. Yamaguchi, S. Sen, A. Morita, and T. Tahara, *J. Chem. Phys.*, **2010**, *132*, 144701.
37. S. Yamaguchi and T. Tahara, *J. Chem. Phys.*, **2008**, *129*, 101102.

38. A. Ghosh, M. Smits, J. Bredenbeck, N. Dijkhuizen, and M. Bonn, *Rev. Sci. Instrum.,* **2008**, *79*, 093907.
39. Z. Zhang, L. Piatkowski, H. J. Bakker, and M. Bonn, *Nature Chem.,* **2011,** *3*, 888.
40. J. Bredenbeck, A. Ghosh, M. Smits, and M. Bonn, *J. Am. Chem. Soc.,* **2008**, *130*, 2152.
41. J. Bredenbeck, A. Ghosh, H.-K. NieQnhuys, and M. Bonn, *Acc. Chem. Res.,* **2009**, *42*, 1332.
42. https://en.wikipedia.org/wiki/Second-harmonic_generation
43. O. N. Slyadneva, M. N. Slyadnev, V. M. Tsukanova, T. Inoue, A. Harata, and T. Ogawa, *Langmuir*, **1999**, *15*, 8651.
44. M. Sato, A. Harata, Y. Hatano, T. Ogawa, T. Kaieda, K. Ohmukai, and H. Kawazumi, *J. Phys. Chem. B*, **2004,** *108*, 12111.
45. M. Sato, T. Kaieda, K. Ohmukai, H. Kawazumi, A. Harata, and T. Ogawa, *J. Phys. Chem. B*, **2000,** *104*, 9873.
46. M. Sato, H. Akagishi, A. Harata, and T. Ogawa, *Langmuir*, **2001,** *17*, 8167.
47. J. M. Perera and G. W. Stevens, *Anal. Bioanal. Chem.*, **2009**, *395*, 1019.
48. S. Tsukahara, *Anal. Chim. Acta.*, **2006**, *556*, 16.
49. H. Nagatani and T. Sagara, *Anal. Sci.*, **2007**, *23*, 1041.
50. I. Benjamin, *Chem. Rev.*, **2006**, *106*, 1212.
51. https://en.wikipedia.org/wiki/Confocal_microscopy.
52. J. B. Pawley, *"Handbook of Biological Confocal Microscopy"*, 3rd ed., **2006,** Chap. 1, Science+Business Media, LLC, New York.
53. S. Nie, D. T. Chiu, and R. N. Zare, *Opt. Lett.*, **1994**, *266*, 1018.
54. Y. Kitazumi and T. Kakiuchi, *Langmuir*, **2009**, *25(18)*, 10829.
55. J. W. Blunt, *Nature Chem.*, **2010**, *2*, 799.
56. M. Schrader, M. Kozubek, S. W. Hell, and T. Wilson, *Opt. Lett.*, **1997**, *22*, 436.
57. V. Hischfeld and C. G. Hübner, *Rev. Sci. Instrum.*, **2010**, *81*, 113705.
58. S. Selci, F. R. Bertani and L. Ferrari, *AIP Adv.*, **2011**, *1*, 032143.
59. B. S. Chun, K. Kim, and D. Gweon, *Rev. Sci. Instrum.*, **2009**, *80*, 073706.
60. Y.-Q. Li, S. Sasaki, T. Inoue, A. Harata, and T. Ogawa, *Appl. Spectrosc.*, **1998,** *52*, 1111.

61. Y.-Q. Li, T. Inoue, A. Harata, and T. Ogawa, *Instrum. Sci. Technol.,* **1999**, *27(3),* 159.
62. Y.-Q. Li, *Langmuir*, **1999**, *15,* 3035.
63. X-.Y. Zheng, A. H*arata,* and T. Ogawa, *Chem. Phys. Lett.*, **2000**, *316,* 6.
64. X-.Y. Zheng, A. Harata, and T. Ogawa, *Spectrochim. Acta, Part A,* **2001**, *57,* 315.
65. X.-Y. Zheng, M. Wachi, A. Harata, and Y. Hanato, *Spectrochim. Acta, Part A,* **2004**, *60,* 1085.
66. X.-Y. Zheng and A. Harata, *Anal. Sci.,* **2001**, *17,* 131.
67. Y.-Q. Li, S. Sasaki, T. Inoue, A. Harata, and T. Ogawa, *Laser. Chem.*, **1998,** *17,* 175.
68. M. N. Slyadnev, T. Inoue, A. Harata, and T. Ogawa, *Colloids Surf., A,* **2000**, *164*, 155.
69. B. T. Mmereki, and D. J. Donaldson, *Phys. Chem. Chem. Phys.*, **2002**, *4*, 4186.
70. J. Han and K. Burgess, *Chem. Rev.,* **2010**, *110*, 2709.
71. A. A. Venn, E. Tambutté, S. Lotto, D. Zoccola, D. Allemand, S. and Tambutté, *PNAS*, **2009**, *106(39)*, 16574.
72. N. Boens, W. Qin, M. Baruah, W. M. De Borggraeve, A. Filarowski, N. Smisdom, M. Ameloot, L. Crovetto, E. M. Talavera, and J. M. Alvarez-Pez, *Chem. Eur. J.*, **2011**, *17*, 10924.
73. https://en.wikipedia.org/wiki/BODIPY
74. S. Chen, Y. Hong, Y. Liu, J. Liu, C. W. T. Leung, M. Li, R. T. K. Kwok, E. Zhao, H. W. Y. Lam, Y. Yu, and B. Z. Tang, *J. Am. Chem. Soc.*, **2013**, *135*, 4926.
75. M. J. Marín, F. Galindo, P. Thomas, and D. A. Russell, *Angew. Chem. Int. Ed.*, **2012**, *51*, 9657.
76. K. Zhou, Y. Wang, X. Huang, K. Luby-Phelps, B. D. Sumer, and J. Gao, *Angew. Chem.*, **2011**, *123*, 6233.
77. K. Zhou, H. Liu, S. Zhang, X. Huang, Y. Wang, G. Huang, B. D. Sumer, and J. Gao, *J. Am. Chem. Soc.*, **2012**, *134*, 7803.
78. J. Lei, L. Wang, and J. Zhang, *Chem. Commun.,* **2010**, *46*, 8445.
79. S. Wu, Z. Li, J. Han, and S. Han, *Chem. Commun.,* **2011**, *47,* 11276.
80. H. Sun, K. Almdal, and T. L. Andresen, *Chem. Commun.,* **2011**, *47*, 5268.
81. W. Shi, X. Li, and H. Ma, *Angew. Chem. Int. Ed.,* **2012**, *51*, 6432.

82. Y.-H. Chan, C. Wu, F. Ye, Y. Jin, P. B. Smith, and D. T. Chiu, *Anal. Chem.*, **2011**, *83*, 1448.
83. H.-S. Peng, J. A. Stolwijk, L.-N. Sun, J. Wegener, and O. S. Wolfbeis, *Angew. Chem. Int. Ed.*, **2010**, *49*, 4246.
84. L. Albertazzi, B. Storti, L. Marchetti, and F. Beltram, *J. Am. Chem. Soc.*, **2010**, *132*, 18158.
85. M. Tantama, Y. P. Hung, and G. Yellen, *J. Am. Chem. Soc.*, **2011**, *133*, 10034.

# CHAPTER 2 Obtaining Fluorescence Spectra of Soluble Molecules at the Air/Water Interface with a Confocal Fluorescence Microscope

## 2.1 Introduction

The air/water interface is a universal but unique region. It is greatly important to understand the air/water interface in physical, analytical and environmental chemistry. One common way for understanding the air/water interface is by means of observing behaviors of soluble molecules adsorbed at the air/water interface. Molecular dynamics is often used to theoretically analyze physical movements of atoms or molecules at the air/water interface based on computer simulation. But it is still difficult to study soluble molecules adsorbed at the air/water interface in an experimental way because of two difficulties. One is that it is difficult to distinguish optical signals generated at the air/water interface from those in the water bulk, namely surface-selectivity. The other is that it is difficult to capture extremely weak optical signals generated at the air/water interface, namely surface-sensitivity. To date, second harmonic generation[1], vibrational sum-frequency generation[2], and two-photon ionization[3] are three current analytical methods for experimentally studying soluble molecules adsorbed at the air/water interface. However, these surface-selective spectroscopic methods lack good sensitivity to work under $10^{-2}$ of a surface coverage of the probe molecules.

In our research group, a confocal fluorescence microscope (CFM) has been applied into studying soluble molecules adsorbed at the air/water interface. By using the CFM, fluorescence emissions of water-soluble fluorescent dyes adsorbed at the air/water interface can be obtained even under a surface density of solute molecules of 1-$10^3$ molecule/$\mu m^2$.[4-6] Furthermore, a complete and corrected fluorescence spectrum of rhodamine B (RhB) molecules adsorbed at the air/water interface was also obtained with the CFM.[7] However, it is no longer applicable to use the same method to align the CFM as reported in previous work[4], because the instrumentation for the CFM is partly changed. The way for aligning the CFM has to be revised according to current experimental conditions, for ensuring the best

surface-selectivity and the highest sensitivity of the CFM during measurements. Another deficiency is that the evidence is still insufficient to support that a complete and corrected fluorescence spectrum of RhB molecules adsorbed at the air/water interface has been acquired.[7]

In this work, a new CFM equipment is developed on the basis of preceding experimental conditions, in order to obtain a complete fluorescence spectrum of soluble molecules adsorbed at the air/water interface with the best surface-selectivity and the highest sensitivity. The accuracy and precision during measurements of this CFM are evaluated. A completed and corrected fluorescence spectrum of RhB adsorbed at the air/water interface is confirmed to be successfully obtained. A set of basic parameters for the CFM are obtained.

## 2.2 Experimental

Rhodamine B was purchased from Nacalai (Kyoto, Japan). Sodium chloride and trisodium citrate were purchased from Chameleon (Osaka, Japan). Hydrochloride and sodium hydroxide were purchased from Wako (Osaka, Japan). Methanol was purchased from Kishida (Osaka, Japan). Coumarin 153 was purchased from Sigma-Aldrich (Tokyo, Japan). The purities of these chemical reagents are all over 99.0%, except that HCl has a purity of about 34.0%.

For surface-selective fluorescence measurements, the concentration of RhB aqueous solutions was adjusted to $1.0\times10^{-8}$ M. Water was purified with a water purification system (Milli-Q Academic A10, Millipore). The pH was maintained by mixing 0.1 M HCl and 0.1 M sodium citrate solution in different ratios. A pH meter (D-52, Horiba) was used to monitor the pH. Ionic strength was maintained at 0.1 M with sodium chloride. For bulk fluorescence measurements in organic solvents, the concentration of RhB was adjusted to $1.0\times10^{-5}$ M.

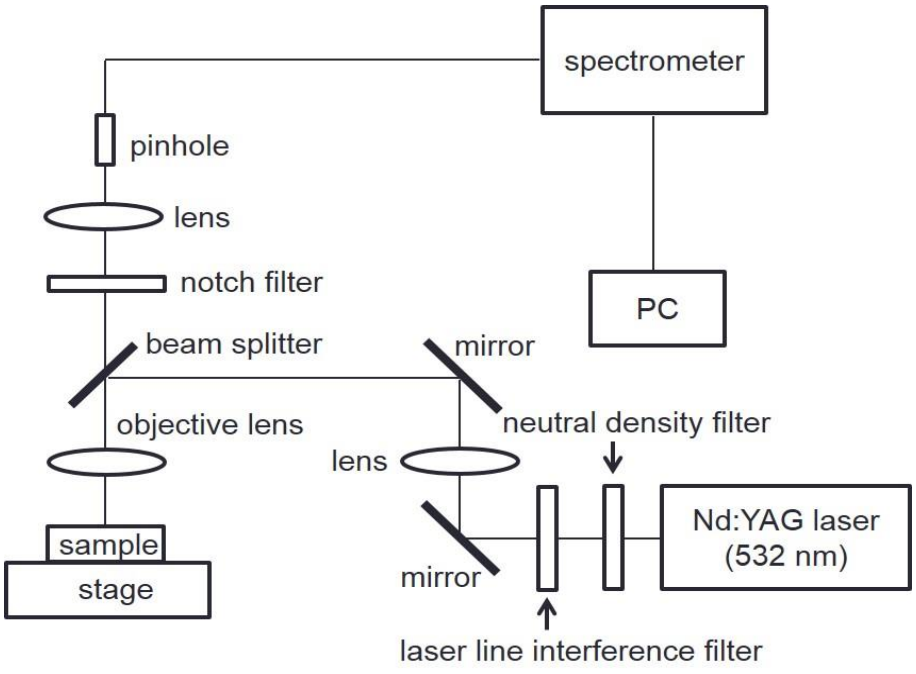


Fig. 2-1 A schematic view of the experimental setup of the CFM

The experimental setup of the CFM is schematically shown in Fig. 2-1. A second harmonic emission of a neodymium-dope yttrium aluminum garnet laser beam (HK-5526-02, Shimadzu) passed through a neutral density filter, a laser line-interference filter (10BPF10-530, Newport), and a pre-focusing lens and reflected downward by a pellicle beamsplitter (03BPL001, Melles Griot). The objective lens (LMPlanApo 150X, Olympus) focused this reflected laser beam on the solution's surface, loaded in a glass cell (diameter, 40 mm; depth, 17 mm). Fluorescence emissions generated at the water surface were collected with the same objective lens and passed through the beamsplitter and a notch filter (550FG05-25, Andover). This fluorescence emission was then focused with a lens (SLSQ-20-50p, Sigma Koki) into a fiber (diameter, 200 μm) connected to a spectroscope (PMA-100, Hamamatsu) under the condition of an exit slit width of 10 μm, an entrance slit width of 100 μm, and an accumulation time of 20 s. The controller reading for magnifying the responses of photons in the spectrometer is between 0.00-3.00**.** The spectroscope was equipped with a grating with 600 g/mm of ruling and 300 nm of blazing wavelength. The fluorescence emission spectrum was transferred to a personal computer and analyzed using software (U8167-02, Ver. 1.3.0).

The fluorescence spectra of RhB at the air/water interface were acquired under conditions of rightly focusing the laser at the air/water interface. The wavenumber axis of the CFM was calibrated with the emission lines of a mercury lamp (L937-01, Hamamatsu), and the fluorescence spectra were corrected by a standard light source (ESC-333, Jasco) and comparing a spectrum observed with the CFM to that obtained with a calibrated spectrofluorometer (FP-6600, Jasco).

The fluorescence spectra of RhB in the bulk were obtained with the spectrofluorometer. A quartz cell (optical path, 1 cm) was used. The measurement conditions of the spectrofluorometer are as follows: excitation slit width, 3 nm; emission slit width, 6 nm; excitation wavelength, 532 nm.

For the experiment of time dependence on fluorescence intensity, the concentration of RhB

aqueous solution is adjusted to $1.8\times10^{-8}$ mol/L. The intensity of fluorescence emission of RhB aqueous solution at 572 nm was selected as the intensity function of concentrations, and was measured every 2 minutes.

For the experiment of the concentration dependence on fluorescence intensity, four different concentrations of the RhB aqueous solutions ($1.8\times10^{-9}$ mol/L, $3.5\times10^{-9}$ mol/L, $1.8\times10^{-8}$ mol/L, and $3.5\times10^{-8}$ mol/L) were measured with the spectrometer and the CFM, respectively. The intensity of fluorescence emission at 572 nm was selected as the dependence of concentrations. Each concentration of RhB solutions was measured five parallel times.

For the experiment of depth resolution of the CFM, that the laser exciting light is rightly focusing on the air/water interface is defined as 0 μm; the direction of moving toward the water phase is defined positive, whereas that of moving toward the gas phase is regarded as negative. The fluorescence spectra at 5 μm, 10 μm, 15 μm, 20 μm, -5 μm, -10 μm, -15 μm, and -20 μm were obtained, respectively. All of the experiments described above were performed at room temperature.

## 2.3 Results and Discussion

### 2.3.1 Fluorescence Spectra at the Air/Water Interface

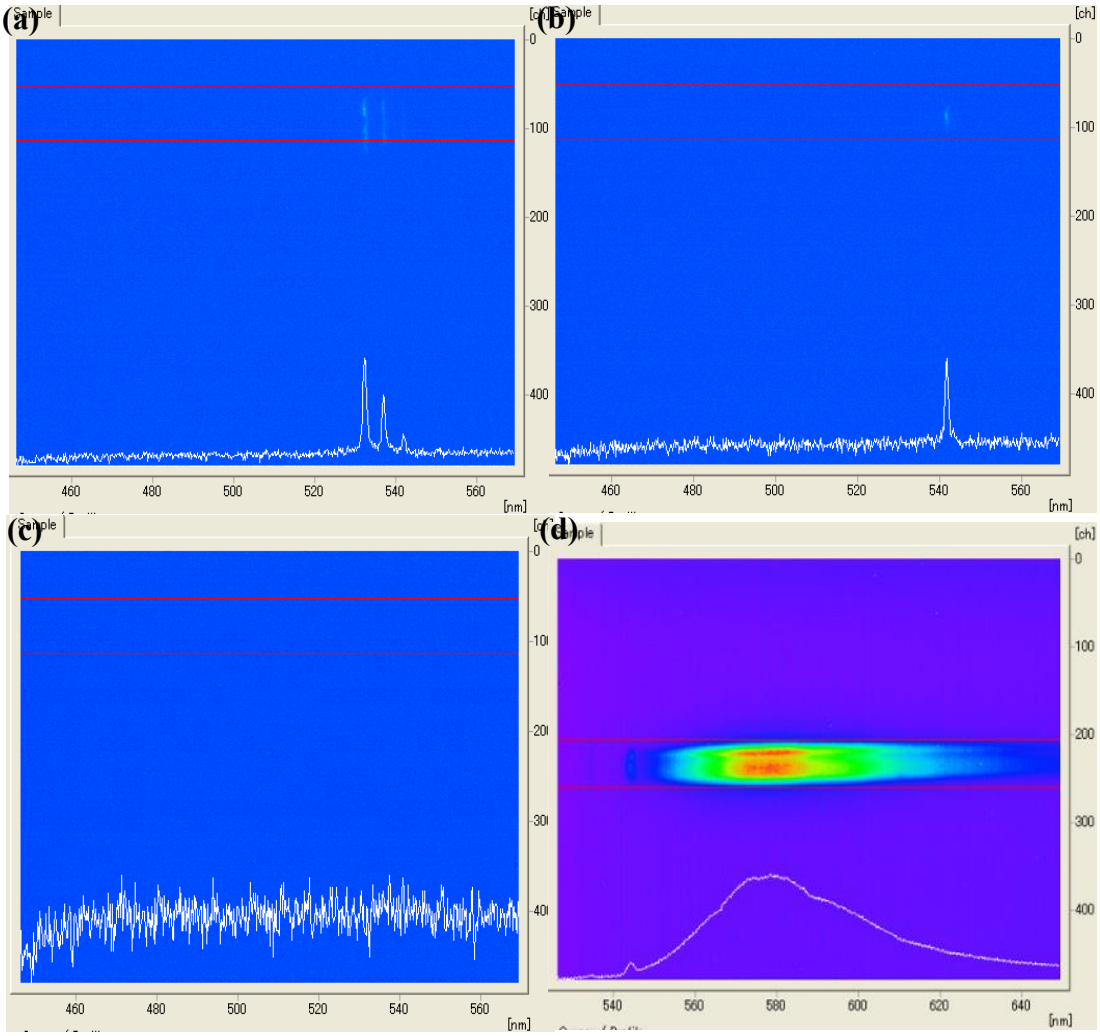


Fig. 2-2(a) The laser line of 532 nm and its two satellite lines of 536 nm and 542 nm; (b) The satellite line of 542 nm; (c) The spectrum of the CFM after alignment but before excitation; (d) The fluorescence spectrum of RhB molecules when the CFM is well aligned

The CFM has been effectively applied to obtain fluorescence emissions of soluble molecules adsorbed at the air/water interface surface-selectively [6]. However, before measurement, it is inevitable to align the CFM, for focusing the laser beam rightly on the air/water interface,

and for exactly collecting fluorescence emissions generated at the air/water interface. The instrumentation for the CFM is fundamentally the same with that reported previously.[4] The biggest difference is that the original light source of CW argon ion laser (Lexel Model 95-4: 1.7 W for 488.0 nm) has been replace with the neodymium-dope yttrium aluminum garnet laser.

The new alignment process for the CFM is shown in Fig. 2-2, which is slightly different from that reported previously.[4] Fig. 2-2(a) shows the laser line of 532 nm and its two satellite lines of 536 nm and 542 nm. As we can see, the peak at 542 nm is shorter than that at 536 nm. Therefore, it is judicious to select the satellite line of 542 nm as the reference line to align the CFM. Fig. 2-2(b) shows the single satellite of 542 nm after the other two lines of 532 nm and 536 nm were filtered. As we consider, the appearance of this tall and narrow peak at 542 nm confirms a good alignment of the CFM. Fig. 2-2(c) shows the spectrum of the CFM after alignment but before excitation. After we set the laser line-interference filter to this well aligned CFM, the peak at 542 nm disappears, which means the satellite line of 542 nm was successfully filtered by this filter. After this, the laser of 532 nm was started to excite the RhB molecules adsorbed the air/water interface. Fig. 2-2(d) shows the fluorescence spectrum of RhB molecules after the CFM is well aligned. Although the evidence is insufficient to support this inference, the acquirement of a clear and complete fluorescence spectrum similar to that of RhB is confirmed. It is concluded that the CFM was aligned well and can be used to obtained fluorescence spectrum of soluble molecules.

The fluorescence spectrum of RhB adsorbed at the air/water interface was successfully acquired with this well aligned CFM. This was evidenced by Fig. 2-3. Fig. 2-3 shows the fluorescence spectra of RhB aqueous solutions measured with different laser focus positions along the z-axis direction. The intensity of fluorescence was not normalized and not smoothed: these fluorescence spectra were all raw data acquired with a CFM. When the laser beam was rightly focused at the air/water interface (0 μm), a broad and strong peak at 584 nm was observed, substantially different from the other peaks. This accords with the common

sense of the surface enrichment of RhB. So this fluorescence spectrum was attributed to that of RhB adsorbed at the air/water interface. When the laser beam was focused under 200 μm, 500 μm, 700 μm and 1000 μm downward the solution surface, the strong and broad peak turned into a broad and weak peak at 579 nm. These fluorescence spectra were attributed to that of RhB in the water bulk.

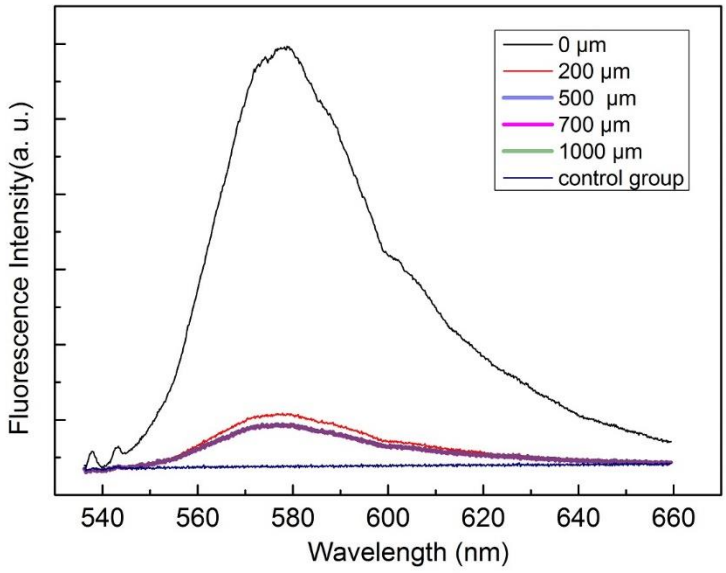


Fig. 2-3 Fluorescence spectrum of RhB molecules at the water surface and in bulk solution by using a CFM

### 2.3.2 Correction of Fluorescence Spectra

Although the complete fluorescence spectrum of RhB molecules adsorbed at the air/water interface was acquired, it is still necessary to correct this fluorescence spectrum, in order to remove wavelength-dependent instrumental effects mainly caused by the spectrometer in the CFM. However, there is no convincing evidence in support of a corrected fluorescence spectra of soluble molecules adsorbed at the air/water interface measured with the CFM in the past work[7].

The effects of smoothing orders on fluorescence spectra measured with the CFM was first evaluated and shown in Fig. 2-4. Raw fluorescence spectra measured with the CFM are often required to be smoothened to remove burrs caused by noise during measurement. In order to optimize the smoothing order, the same concentration of RhB solutions was measured under different smoothing orders. As shown in Fig. 2-4, the smoothing order of 4 is found to be the optimal one in which not only the burrs were almost removed, but also the original shape of

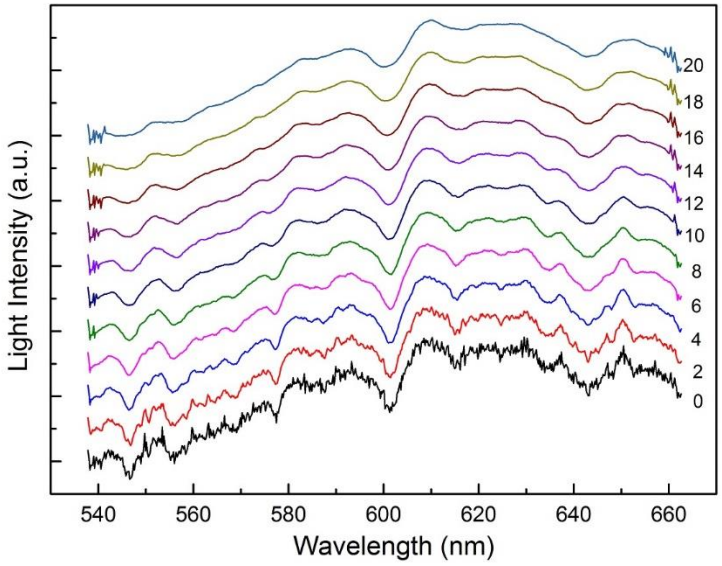


Fig. 2-4 The effects of smoothing orders on fluorescence spectra measured with the CFM

fluorescence spectrum remains unchanged. For the sake of convenience, each fluorescence spectrum measured with the CFM has to be smoothed with an order of 5 before extracting to utilize.

Since the wavelength axis of the spectrometer in the CFM was corrected with the emission lines of mercury lamp, the accuracy for the spectrometer in the CFM is guaranteed only partially. On the other hand, the precision of the spectrometer in the CFM is also essential to be evaluated seriously.

The precision of the CFM when measuring fluorescence peak wavelengths was also evaluated. The result is shown in Tab.2-1, which shows fluorescence peak wavelengths of RhB molecules adsorbed at the air/water interface measured with the CFM for five times. The precision of the CFM for measuring fluorescence peak wavelengths of RhB molecules at the air/water interface is high. The RSD% for the RhB solutions with different concentrations of $1.8 \times 10^{-8}$ mol/L, $3.5 \times 10^{-8}$ mol/L, and $1.8 \times 10^{-9}$ mol/L, are 0.00739%, 0.171%, and 0.0691%, after each fluorescence spectrum was smoothened with an order of 5.

Tab. 2-1 Fluorescence peak wavelengths of RhB molecules adsorbed at the air/water interface measured with the CFM for five times

| Concentrations of RhB (mol/L) | Mean(before smoothing) | Mean(after smoothing) | RSD%(before smoothing) | RSD%(after smoothing) |
|---|---|---|---|---|
| $1.8 \times 10^{-8}$ | 574.1 | 573.1 | 0.102 | 0.0739 |
| $3.5 \times 10^{-8}$ | 572.8 | 571.8 | 0.262 | 0.171 |
| $1.8 \times 10^{-9}$ | 570.2 | 570.1 | 0.421 | 0.0691 |

Despite of good accuracy and precision for measuring fluorescence peak wavelengths with the CFM, the fluorescence spectrum measured with the CFM is also required to be corrected strictly. The aim is to eliminate the wavelength-dependent efficiency of the detection system[8], caused by a grating in the spectrometer of the CFM.

The first correction method that we selected is to use a standard light source to correct the fluorescence spectrum measured with the CFM. The spectrometer in the CFM has multiple channels to receive and transmit photons, which indicated in the form of 0-500 ch in the display screen shown in Fig. 2-5. The 19-93 ch, 66-136 ch, 156-228 ch, and 232-341 ch were selected as channels of four independent groups.

In Fig. 2-6 the white light emitting from the standard light source passed through each channel, and was recorded as four respective emission spectrum with the spectrometer in the

CFM. Even though these four emission spectra roughly have the same spectrum shape, a few

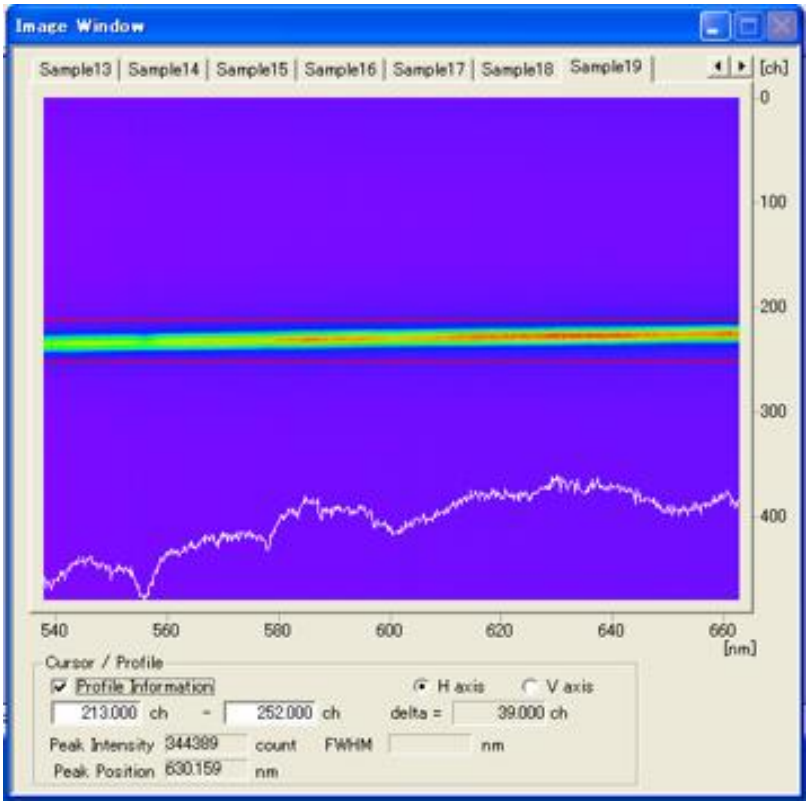


Fig. 2-5 The emission spectrum of standard light source measured with the spectrometer in the CFM

fine differences in these four emission spectra are clear to be observed. It is concluded that different channels (or spectrum in different ch) in this spectrometer has different wavelength-dependent efficiency, and thus has to be corrected independently.

The correcting process is described as follows,

$$\gamma(\lambda) = I(\lambda) / L(\lambda), \tag{2-1}$$

$$C(\lambda) = M(\lambda) / \gamma(\lambda). \tag{2-2}$$

Where,

$L(\lambda)$ is the ideal emission spectrum of standard light source; $I(\lambda)$ is the emission spectrum of standard light source measured with a fixed channel of the spectrometer under in the CFM; $\gamma(\lambda)$ is the correction factors of the fixed channel of the spectrometer in the CFM; $M(\lambda)$ and $C(\lambda)$ are measured and corrected fluorescence spectrum of RhB molecules adsorbed at the air/water interface measured with the fixed channel of the spectrometer in the CFM.

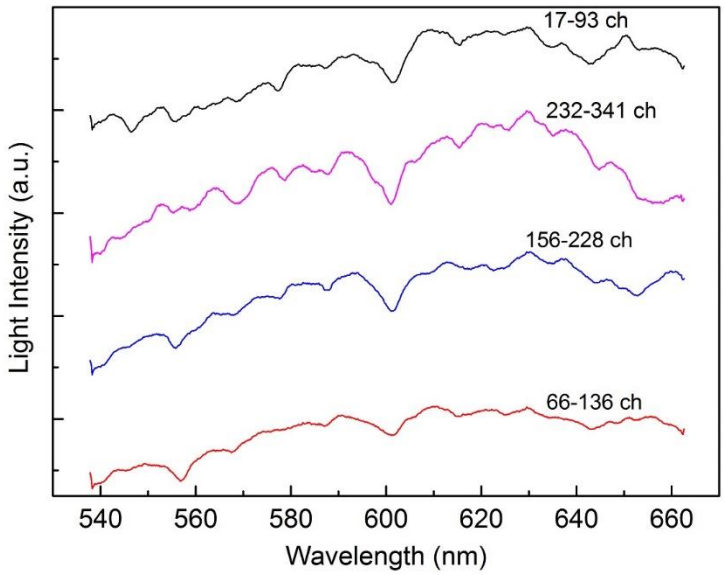


Fig. 2-6 The effects of pixel positions on emission spectra of standard light source

Although this correction method of using standard light source was used to corrected fluorescence spectrum of RhB molecules adsorbed at the air/water interface measured with the CFM, no satisfying result of corrected fluorescence spectrum was finally acquired. The reason may be that the standard light source is improper to correct a multichannel spectrometer. It is difficult to fix a channel (or pixel region) in the spectrometer for each measurement.

Thanks to unavailability of the correction method of standard light source, another correction method with a corrected spectrofluometer was used to correct the fluorescence spectrum

measured with the CFM. This method is based on comparing a spectrum observed with the CFM to that obtained with the calibrated spectrofluorometer[8], and its principle is described as follows,

$$\gamma(\lambda) = B(\lambda) / B'(\lambda) \tag{2-3}$$

$$S'(\lambda) = S(\lambda) \times \gamma(\lambda) \tag{2-4}$$

Where,

$B(\lambda)$ is the bulk fluorescence spectrum measured with the corrected spectrofluometer; $B'(\lambda)$ is the bulk spectrum measured with the CFM; $\gamma(\lambda)$ is the correction factors of the spectrometer in the CFM; $S(\lambda)$ is surface fluorescence spectrum measured with the CFM; $S'(\lambda)$ is the final corrected surface fluorescence spectrum measured with the CFM.

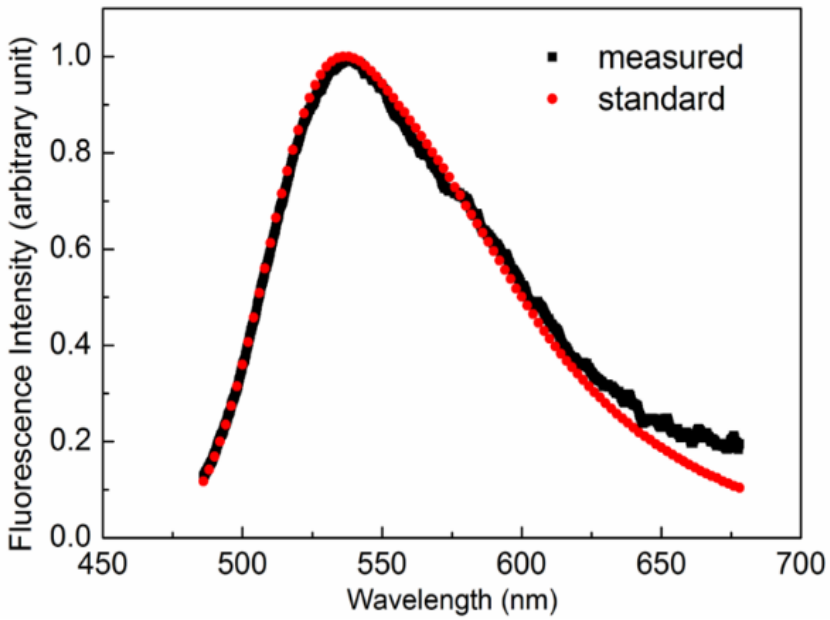


Fig. 2-7 Standard and measured fluorescence emission spectra of courmarine 153 in methanol solution with concentration of $10^{-6}$ mol/L

The corrected spectrofluorometer in this correction method was also proved to be a

sufficiently corrected with standard substances. Figure 2-7 shows measured and standard fluorescence emission spectra of courmarin 153 in methanol solution with a concentration of $10^{-6}$ mol/L. The measured curve is the fluorescence emission spectrum of courmarin 153 in methanol solution of $10^{-6}$ M measured with this corrected spectrofluorometer, whereas the standard one is directly obtained from the textbook.[8] It was found obviously that the two curves overlapped well in region of 480~620 nm that we are interested, which gives a strong support for the accuracy of this corrected spectrofluorometer.

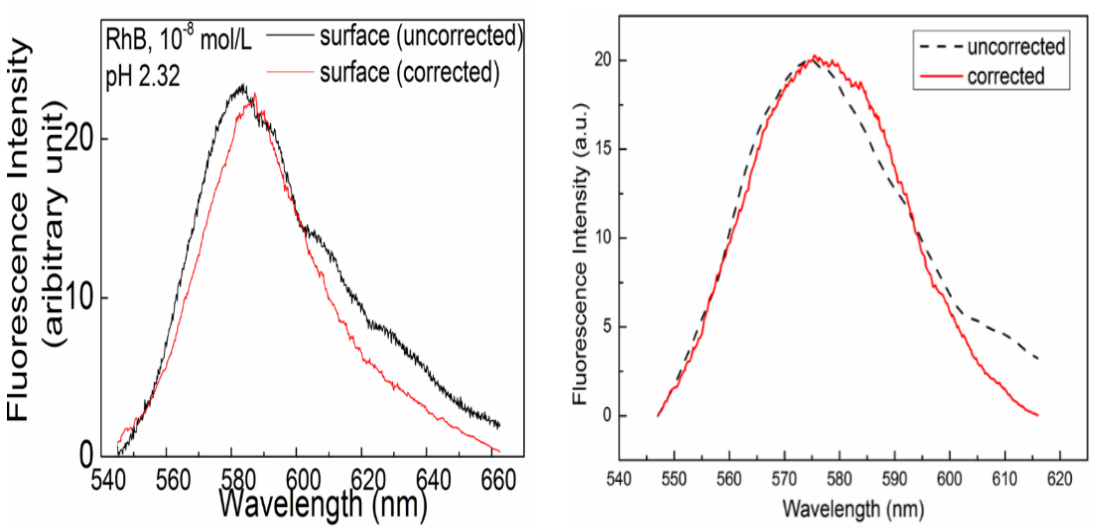


(a) (b)

Fig. 2-8 Fluorescence spectra of RhB at the air/water interface measured with the CFM before and after correction for the first (a) and the second time (b)

Figure 2-8 shows fluorescence spectra of RhB at the air/water interface measured with the CFM before and after correction for the first (a) and the second time (b). The corrected fluorescence spectra of RhB at the air/water interface in the two figures above show a consistent result of red shift, in contrast to those uncorrected. The only difference between Fig. 2-8(a) and Fig. 2-8(b) is channels, or pix positions displayed in the screen shown in Fig. 2-5, in the spectrometer of the CFM. In Fig. 2-8(a), the pixel positions were fixed approximately between 200-250; In Fig. 2-8(b), they were fixed exactly between 80-100.

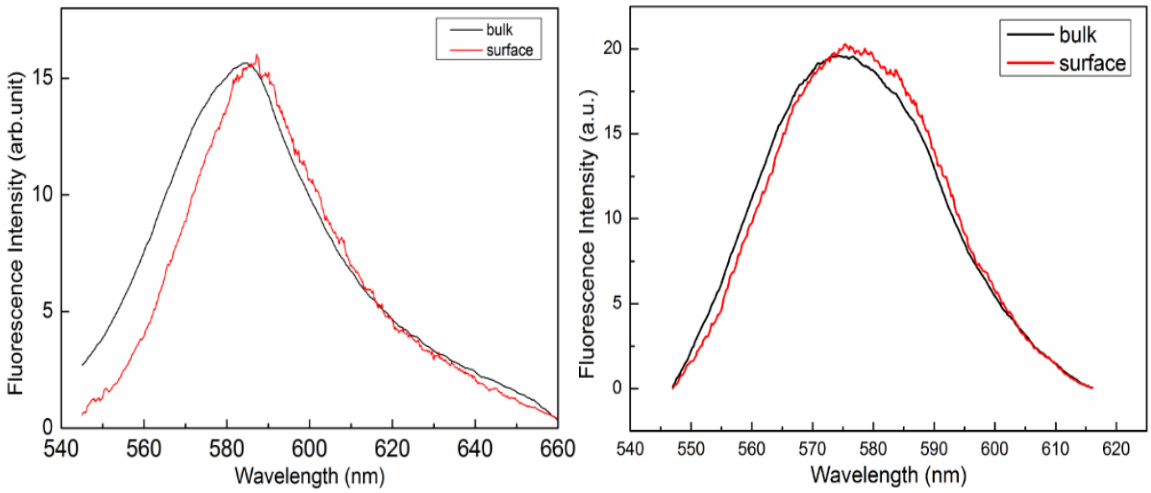


Fig. 2-9 Fluorescence spectra of RhB at the air/water interface and in bulk for the first time (a) and the second time (b)

Figure 2-9 shows two corrected fluorescence spectra of RhB at the air/water interface and in bulk. Even with two independent experiments, both figures show a nearly common result. A several-nanometer red shift from the bulk fluorescence spectrum was clearly observed. This result indicates that the air/water interface has an environment a bit different from that of the bulk.

Briefly, it is reliable to correct the fluorescence spectrum measured with CFM with such a spectrofluorometer, aiming at eliminating the wavelength-dependent efficiency of the detection system caused by the grating in the spectrometer of the CFM. The correction factors $\gamma(\lambda)$ of the spectrometer in 80-100 pixel position in the CFM were also obtained and reserved in the appendix 1 of this dissertation. Since the correction factors $\gamma(\lambda)$ is still available in future research, it facilitates future work in the aspect of spectrum correction.

### 2.3.3 Other Performances of the Confocal Fluorescence Microscope

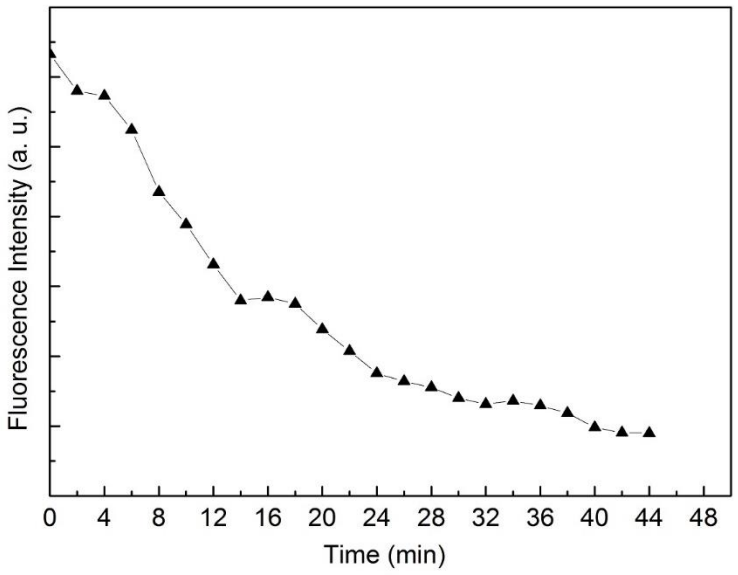


Fig. 2-10 The time dependence on fluorescence intensity of RhB molecules adsorbed at the air/water interface measured with the CFM

The time dependence on fluorescence intensity of soluble molecules adsorbed at the air/water interface measured with the CFM is revealed. Figure 2-10 shows such a result in a period of 44 minutes. As we can see, the fluorescence intensity decreases with time as a whole. Due to evaporation of water in the RhB solution, the liquid level of the RhB solution descends gradually until the laser no longer focus on the air/water interface. When the laser no longer focus on the air/water interface, the fluorescence intensity measured with the CFM drops substantially without doubt, because of surface enrichment of RhB molecules. This result provides a significant guidance when the CFM is used to measure the fluorescence spectrum of soluble molecules adsorbed at the air/water interface, especially in the aspect of measuring the fluorescence spectrum at the air/water interface in time.

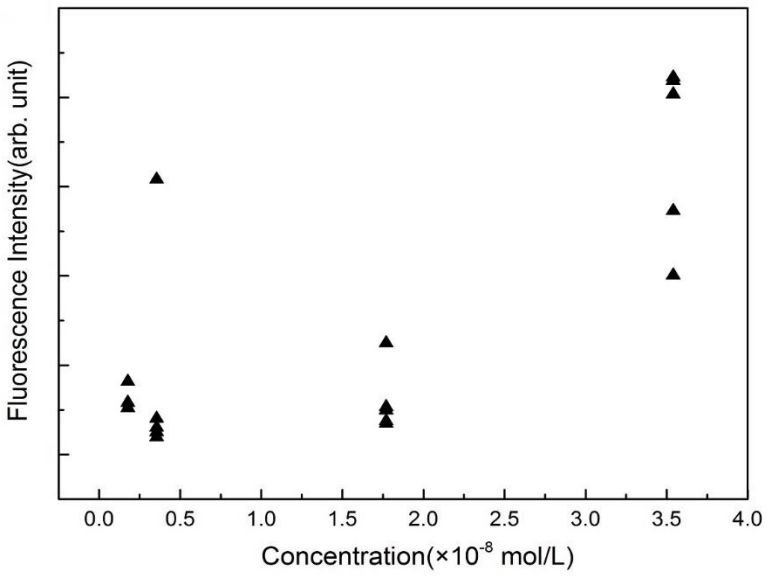


Fig. 2-11 The relationship between the concentration and the fluorescence intensity measured with the CFM

The concentration dependence on the fluorescence intensity of soluble molecules adsorbed at the air/water interface measured with in the CFM was also investigated. As shown in Fig. 2-11, no expected linear relationship was obviously observed between the concentration and the fluorescence intensity measured with the CFM, which is inconsistent with that reported in the previous work[6]. Here we note that, the fluorescence intensity is from RhB molecules adsorbed at the air/water interface, whereas the concentration is from RhB molecules in the water bulk.

Additionally, the precision for measuring the fluorescence intensity each time is also much lower than expected. In other words, the fluorescence intensity measured each time fluctuates seriously, even for the same concentration of RhB aqueous solution. Unlike the peak wavelength shown in Tab. 2-1, it is difficult to take advantage of the fluorescence intensity measured with the CFM as one essential variable to study the air/water interface under current instrumental conditions.

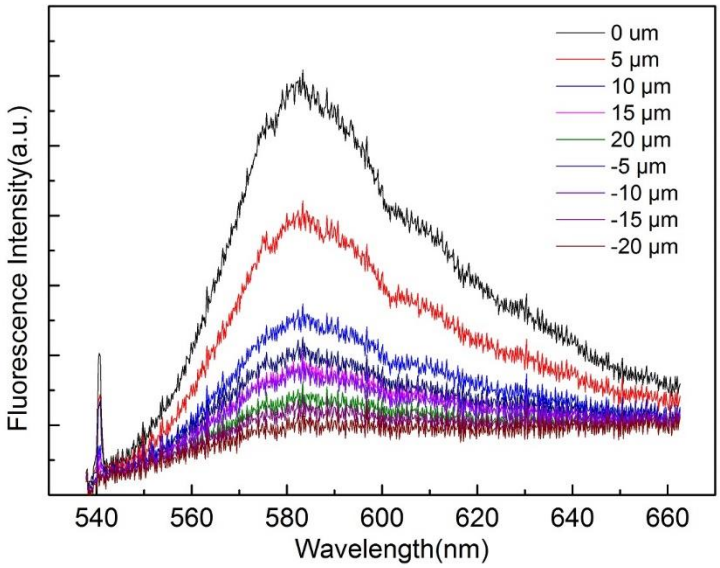


Fig. 2-12 The depth resolution of the CFM

The depth resolution for the CFM is also investigated. The result is shown through Fig. 2-12. Moving the stage towards the liquid phase is defined the positive direction. When the laser exciting light focuses on the point 5 μm downward from the air/water interface, despite of decreasing of fluorescence intensity, the shape of fluorescence spectrum measured at this point has not changed obviously. So it is high likely to be the fluorescence spectrum at the air/water interface. However, when the laser exciting light focuses on the point 10 μm downward from the air/water interface, the fluorescence spectrum obtained at this point is probably not the one at the air/water interface, because the shape of fluorescence spectrum has changed a bit. When the laser exciting light focuses on the point 5 μm upwarod from the air/water interface (-5 μm), the fluorescence spectrum obtained at this point is probably not the one at the air/water interface, because the shape of fluorescence spectrum has changed a lot.

Therefore, in order to obtain the fluorescence spectrum of soluble molecules adsorbed at the air/water interface, the focus position $f$ of laser beam should be -5 μm < $f$ <10 μm. Otherwise,

the fluorescence spectrum of soluble molecules in the water bulk, or no fluorescence spectrum would be acquired, due to a dislocated focus position of laser beam. This result has its reference value in adjusting the focus position of laser beam, when we operate the CFM to obtain the fluorescence spectrum of soluble molecules adsorbed at the air/water interface.

## 2.4 Conclusion

It is essential to align the CFM before measurement in order to ensure its best surface-selectivity and the highest sensitivity. In this chapter, a revised way for aligning the CFM is introduced. And, the complete fluorescence spectrum of RhB molecules adsorbed at the air/water interface is also obtained after aligning the CFM.

The accuracy and precision of measurements with the CFM were evaluated, and a variety of methods was tried be corrected the fluorescence spectrum measured with the CFM. The fluorescence spectrum measured with the CFM was lastly corrected with the method of comparing a spectrum observed with the CFM to that obtained with the calibrated spectrofluorometer. A completed and corrected fluorescence spectrum of RhB molecules adsorbed at the air/water interface was thus attained.

A number of basic parameters of the CFM were also measured, including the time dependency of fluorescence density in the CFM, the solution concentration dependence of fluorescence intensity in the CFM, the depth resolution for the CFM, and optimal smoothing orders. These basic parameters help us to know the CFM more and better, and provide guidance for our future research.

## References


1. O. N. Slyadneva, M. N. Slyadnev, V. M. Tsukanova, T. Inoue, A. Harata, and T. Ogawa, Langmuir, **1999**, *15*, 8651.
2. Y. R. Shen and V. Ostroverkhov, *Chem. Rev.*, **2006**, *106*, 1140.
3. M. Sato, T. Kaieda, K. Ohmukai, H. Kawazumi, A. Harata, and T. Ogawa, *J. Phys. Chem. B,* **2000,** *104,* 9873.
4. Y.-Q. Li, T. Inoue, A. Harata, and T. Ogawa, *Instrum. Sci. Technol.*, **1999**, *27,* 159.
5. Y.-Q. Li, M. N. Slyadnev, T. Inoue, A. Harata, and T. Ogawa, *Langmuir*, **1999**, *15,* 3035.
6. X.-Y. Zheng, A. Harata, and T. Ogawa, *Spectrochim. Acta, Part A*, **2001**, *57*, 315.
7. Y. Imanishi, "*Development of a pH-determination Method at the Air/water Interface with a Confocal Fluorescence Microscope*", **2012**, unpublished master thesis, Kyushu University.
8. J. R. Lakowicz, "*Principles of Fluorescence Spectroscopy*", 3rd ed., **2006**, Chap. 2, Springer Science+Business Media, LLC, New York.

# CHAPTER 3 Estimating pH at the Air/Water Interface with the Confocal Fluorescence Microscope

## 3.1 Introduction

Understanding the air/water interface is of great importance in physical, analytical, and environmental chemistry.[1] Since the pH is an important physical and chemical property, the pH at the air/water interface has been a recent study topic. Interestingly, the pH at the air/water interface is different from that in a bulk solution. As is known to all, in pure water the ionization equilibrium of water molecules is $2H_2O = H_3O^+ + OH^-$. The concentrations of hydroniums are considered to be about $10^{-7}$ M, namely pH 7. However, since the air/water interface is a thin and unique region with distinct anisotropy across it, the composition and structure of species appear at this interface in a unique way, and thus may lead into an specific ionization equilibrium for the air/water interface.[2] Another point of view also considers that hydroniums produced by water molecules may form the electric double layer at the air/water interface.[3] Which ion, hydronium or hydroxide, is more concentrated at the air/water interface is still a controversial question. To date, a wide range of analytical methods have been applied to studying the pH at the air/water interface. Molecular dynamic simulations concluded that the air/water interface is about 2.2 units more acidic than that in bulk solution.[4] Tabe *et al*. calculated the acid–base equilibrium constant ($pK_a$) of trimethylamine at the water surface with quantum mechanics/molecular mechanics and thermodynamic integration calculations, and elucidated the observed pKa shift at the water surface.[5] Electrophoresis[6-7] and electrospray mass spectrometry[8] were also reported to show that at the air/water interface, pH is more basic than that in bulk solution.

Commonly used experimental methods for studying the water surface pH are spectroscopic methods: second-harmonic generation,[9-11] vibrational sum-frequency generation,[12-14] heterodyne-detected electronic sum-frequency generation,[15] and two-photo ionization.[16] were used to clarify the acidity of the air/water interface. Mostly, they showed that the water surface pH is more acidic. However, these surface-selective spectroscopic methods lack good

sensitivity to work under $10^{-2}$ of a surface coverage of the probe molecules. A spectroscopic method with a higher sensitivity is required to drastically reduce the effects caused by the probe on the pH.

A confocal fluorescence microscope (CFM) was used to observe the fluorescence emission of water-soluble rhodamine dyes adsorbed at the air/water interface even under the surface density of solute molecules, being 1-$10^3$ molecule/$\mu m^2$.[17-19] This was achieved by focusing the 532 nm laser beam on the water surface to obtain fluorescence emission surface selectively with a couple of lenses and a pinhole.

Fluorescent pH indicators are often used to monitor the pH in places such as cells, where pH meters cannot operate.[20] Their fluorescence properties, such as fluorescence intensity and fluorescence peak wavelength, often vary with the pH. Rhodamine B (RhB) dye, a fluorescent pH probe with a pKa of 3.1, has two types of ionic forms in aqueous solutions. As shown in Fig. 3-1, the cationic form ($RhBH^+$) shows a fluorescence peak wavelength at 584 nm, whereas the zwitterionic form ($RhB^{\pm}$) shows it at 578 nm.[21] The surface activity of this dye[1][19] indicates the potential for a good indicator of the pH at the air/water interface.

In this work, CFM was first used to estimate the pH at the air/water interface, and a new pH-determination method at the air/water interface was proposed. A relationship between the pH at the air/water interface and that in bulk solution has been formulated in connection with the adsorption equilibrium and dissociation equilibrium of the dye adsorbed at the air/water interface. The fluorescence spectrum of RhB molecules adsorbed at the air/water interface was correctly acquired. The pH dependence of fluorescence peaks at the air/water interface was examined. The result showed that the fluorescence peak at the air/water interface has a wavelength close to that in ethane-1,2-diol. By means of surface tension experiments, the maximum surface density and adsorption equilibrium constants of $RhBH^+$ and $RhB^{\pm}$ were obtained. A way to determine pH at the air/water interface has been discussed.

## 3.2 Experimental

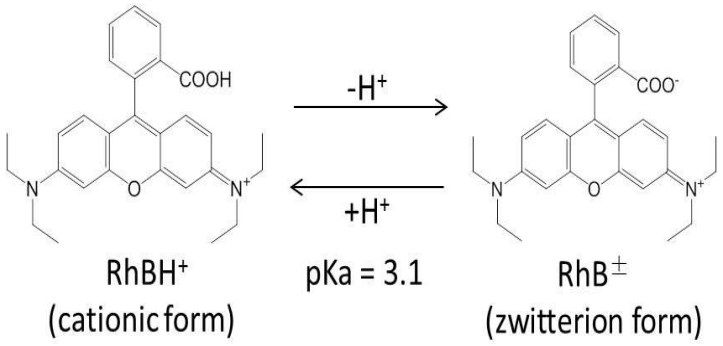


Fig. 3-1 Dissociation equilibrium of RhB in aqueous solution

### 3.2.1 Reagents and chemicals

Rhodamine B was purchased from Nacalai (Kyoto, Japan). Sodium chloride, trisodium citrate, and propane-1,2,3-triol were purchased from Chameleon (Osaka, Japan). Hydrochloride, sodium hydroxide, ethane-1,2-diol, ethanol, and n-propanol were purchased from Wako (Osaka, Japan). Formamide was purchased from Sigma-Aldrich (Tokyo, Japan). 5-(and-6)-carboxyseminaphthorhodafluor-1 was purchased from Molecular Probes (USA). Potassium dihydrogen phosphate was purchased from Wako (Osaka, Japan). Sodium hydrogen phosphate was purchased from Kishida (Osaka, Japan). Citric acid monohydrate was purchase from Wako (Osaka, Japan). The purities of these chemical reagents were all over 99.0%, except that of HCl, which is about 34.0%.

For surface-selective fluorescence measurements, the concentration of RhB aqueous solutions was adjusted to $1.0\times10^{-8}$ M. Water was purified with a water-purification system (Milli-Q Academic A10, Millipore). The pH was maintained by mixing 0.1 M HCl and 0.1 M sodium citrate solution in different ratios. A pH meter (D-52, Horiba) was used to monitor the pH. ionic strength was maintained at 0.1 M with sodium chloride. For bulk fluorescence measurements in organic solvents, the concentration of RhB was adjusted to $1.0\times10^{-5}$ M.

For surface-selective fluorescence measurements, the concentration of SNARF aqueous

solutions was adjusted to $1.0\times10^{-7}$ M. The pH is mainly maintained by mixing 0.1 M potassium dihydrogen phosphate solution and 0.1 M sodium hydrogen phosphate solution in different ratios. Besides, 0.01 M HCl acid solution and 0.01M sodium hydroxide solution was also used for fine adjustment of pH. The other aspects, including water purification, pH meter and ionic strength control, are the same with those in RhB experiments above. The stage position of the laser exciting light rightly focusing on the air/water interface was defined to be 0 μm. The stage was moved toward the liquid phase for 100 μm, 200 μm, and 300 μm., and also moved toward the gas phase for 100 μm.

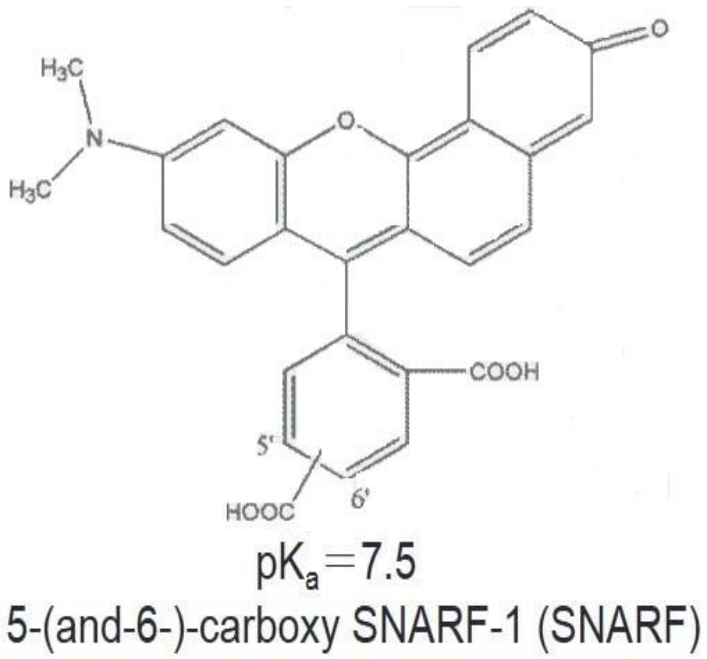


Fig. 3-2 The chemical structure of 5-(and-6-)-carboxy SNARF-1

### 3.2.2 Apparatus

The experimental setup of the CFM is the same as described in chapter 2.

The fluorescence spectra of RhB at the air/water interface were acquired under conditions of rightly focusing the laser at the air/water interface. The wavenumber axis of the CFM was

calibrated with the emission lines of a mercury lamp (L937-01, Hamamatsu), and the fluorescence spectra were corrected by comparing a spectrum observed with the CFM to that obtained with a calibrated spectrofluorometer (FP-6600, Jasco).

The fluorescence spectra of RhB and SNARF in a bulk solution were obtained with the spectrofluorometer. A quartz cell (optical path, 1 cm) was used. The concentration of RhB aqueous solution was adjusted to $1.0\times10^{-8}$ M, whereas that of SNARF aqueous solution to $1.0\times10^{-9}$ M. The measurement conditions of the spectrofluorometer are as follows: excitation slit width, 3 nm; emission slit width, 6 nm; excitation wavelength, 532 nm. All of the experiments described above were performed at room temperature.

The surface tension of RhB aqueous solutions with a variety of pH values was measured with a surface pressure meter (HBM, Kyowa). This meter was based on the Wilhelmy plate method described as follows: a glass plate (24.0 mm × 1.25 mm × 0.3 mm) was immersed into a solution sample. The glass plate was lifted up slowly from this solution sample until its bottom end exactly contacted the solution's surface. The value of force F at this point was wrote down. The surface tension γ was calculated with Eq. (3-1):

$$\gamma = F + dShg \tag{3-1}$$

where $F$ is the value of force at this point displayed in this surface pressure meter (dyne/cm), $d$ is solution density (69.90 dyne/cm, according to water density), $S$ is basal area of the glass plate (24.0 mm × 0.3 mm), $h$ is the depth of glass plate immersing in solution (0.087 m, according to coefficient of elasticity of water), and $g$ is the gravity constant (979.7 cm· $s^{-2}$).

The glass plate was immersed in concentrated sulfuric acid for 12 h before use, in order to obtain a hydrophilic treatment. The concentration of RhB was adjusted to a series of concentrations from $10^{-6}$ M to $10^{-8}$ M by diluting a $10^{-5}$ M RhB aqueous solution. The pH was adjusted to a series of pH values with 0.1 M HCl. The ionic strength was kept at 0.1 M

with sodium chloride. Water and ethanol as standard substances was used to correct the surface pressure meter. The temperature was kept at 25℃.

## 3.3 Results and Discussion

### 3.3.1 A Model of the Air/Water Interface and a pH-Determination Method

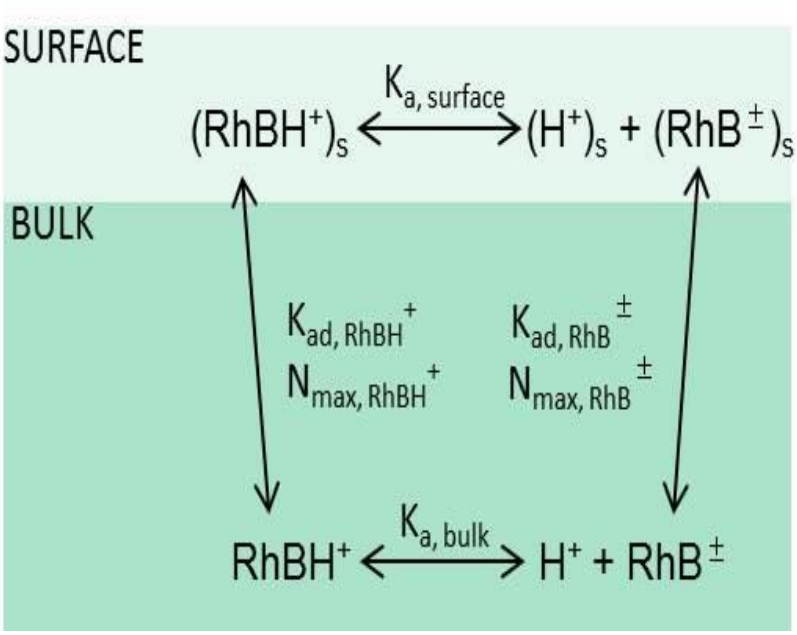


Fig. 3-3 Schematic illustration of the dissociation and adsorption equilibria of RhB molecules at the air/water interface and in bulk.

The air/water interface is a region with a certain thickness of molecular scale in which chemical and physical properties are ensemble-averaged over a certain depth, and gradually change from a liquid phase to a gas phase.[22] Because this region is thin and turbulent, a homogenous region could be expected if a span of time is taken into account. Molecular dynamic simulations[23] yielded the calculation that the air/water interface is an interfacial region not sharp at a microscopic level, with a thickness of about 3.2 Å. Vibration sum-frequency generation experiments[24] also revealed that the thickness of this interfacial region is about 6 Å, judging from the sum-frequency intensity signal.

A model for describing the acid–base dissociation and adsorption equilibria of RhB molecules at the air/water interface and in bulk is shown in Fig. 3-3. An assumption is made that the air/water interface is a thin and homogenous region differing from the bulk. In both

the surface and bulk regions, the acid–base dissociation equilibrium of $RhBH^+$ was considered, in which the dissociation constants, $K_{a,surf}$ and $K_a$, can be different from each other. Between these two regions, the adsorption equilibria of $RhBH^+$ and $RhB^{\pm}$ were considered.

For RhB at the air/water interface, the dissociation constant, $K_{a,surf}$, is given as

$$K_{a,surf} = \frac{[H^+]_s[RhB^{\pm}]_s}{[RhBH^+]_s} = \frac{[H^+]_s N_{RhB^{\pm}}}{N_{RhBH^+}}, \quad (3\text{-}2)$$

Where $N_i$ represents the surface density of protonated or zwitterionic forms of RhB (i = $RhBH^+$ or $RhB^{\pm}$).

For RhB in the bulk, the dissociation constant, $K_a$, is given as

$$K_a = \frac{[H^+]C_{RhB^{\pm}}}{C_{RhBH^+}}, \quad (3\text{-}3)$$

Where $C_i$ is the concentration of i-type forms of RhB.

Assuming that the relationship between the surface density and bulk concentration is represented by the Langmuir isotherm for each chemical form, where co-adsorption occurs, Eq. (3-4) and Eq. (3-5) are acquired:

$$N_{RhB^{\pm}} = \frac{N_{max,RhB^{\pm}} K_{ad,RhB^{\pm}} C_{RhB^{\pm}}}{1 + K_{ad,RhBH^+} C_{RhBH^+} + K_{ad,RhB^{\pm}} C_{RhB^{\pm}}}, \quad (3\text{-}4)$$

$$N_{RhBH^+} = \frac{N_{max,RhBH^+} K_{ad,RhBH^+} C_{RhBH^+}}{1 + K_{ad,RhBH^+} C_{RhBH^+} + K_{ad,RhB^{\pm}} C_{RhB^{\pm}}}, \quad (3\text{-}5)$$

where $N_{max,i}$ is the maximum surface density and $K_{ad,i}$ is the adsorption equilibrium constant of i-type forms of RhB.

From Eq. (3-2), Eq. (3-3), Eq. (3-4), and Eq. (3-5), Eq. (3-6) can be deducted:

$$pH_{surf} - pH = \mathrm{pK_{a,surf}} - \mathrm{pK_a} + \log_{10}\left(\frac{N_{max,RhB^{\pm}} K_{ad,RhB^{\pm}}}{N_{max,RhBH^{+}} K_{ad,RhBH^{+}}}\right). \quad (3\text{-}6)$$

This equation represents the pH difference between the surface and bulk, $\Delta_{pH} = pH_{surf} - pH$, as a constant. This is because all of the parameters in the right-hand side of Eq. (3-5) are determined by the properties of any indicator. If $K_{a,surf}$, $K_a$, $N_{max,RhBH^+}$, $N_{max,RhB^{\pm}}$, $K_{ad,RhBH^+}$, and $K_{ad,RhB^{\pm}}$ are obtained, $pH_{surf}$ can be calculated using Eq. (3-6).

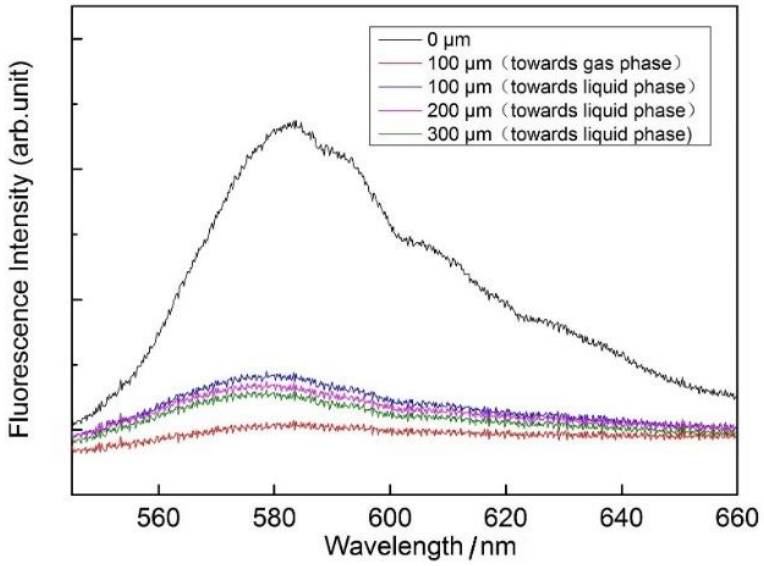


Fig. 3-4 Fluorescence spectra of RhB aqueous solutions measured with different laser focus positions along the depth direction (pH = 2.32)

### 3.3.2 Fluorescence Spectrum of Rhodamine B at the air/water interface

The fluorescence spectrum of RhB molecules adsorbed at the air/water interface was successfully acquired with a CFM. Figure 3-4 shows the fluorescence spectra of RhB aqueous solutions measured with different laser focus positions along the depth direction. The intensity of fluorescence was not normalized and not smoothed: these fluorescence spectra were all raw data acquired with a CFM. When the laser beam was rightly focused at the air/water interface (0 μm), a broad and strong peak at 584 nm was observed. This fluorescence spectrum was attributed to that of RhB adsorbed at the air/water interface. When the laser beam was focused under 100, 200, and 300 μm downward from the solution surface, that strong and broad peak turned into a broad and weak peak at 579 nm. These fluorescence spectra were attributed to that of RhB in bulk. When the laser beam was focused at 100 μm upward from the solution surface in the gas phase, almost no peak was observed.

For the corrected fluorescence spectra of RhB at the air/water interface and in bulk, they have been introduced in Fig. 2-10.

The pH dependence of the fluorescence peak wavelengths of RhB molecules in bulk (see Supporting Information for more detail concerning the mathematical relationship between the fluorescence peak wavenumbers and the pH) is shown in Fig. 3-5. The fluorescence peak wavelength of $RhBH^+$ in bulk solution at a pH lower than 2 and that of a $RhB^{\pm}$ pH higher than 4 were both obtained. The $RhBH^+$ form in bulk solution had a fluorescence peak at 584 nm, while the $RhB^{\pm}$ form had one at 578 nm. Typically, the pKa of RhB is determined with a figure of distribution fraction of $RhBH^+$ or $RhB^{\pm}$ plotted with the pH. The pH that corresponds to 0.5 of the distribution fraction of $RhBH^+$ or $RhB^{\pm}$ in this figure is often considered to the pKa. However, it is also reasonable to directly use a figure of peak wavelengths of RhB plotted with the pH to determine pKa. In this figure, the pH that corresponds to 0.5 of the sum of the peaks wavelength of $RhBH^+$ and $RhB^{\pm}$ is considered to

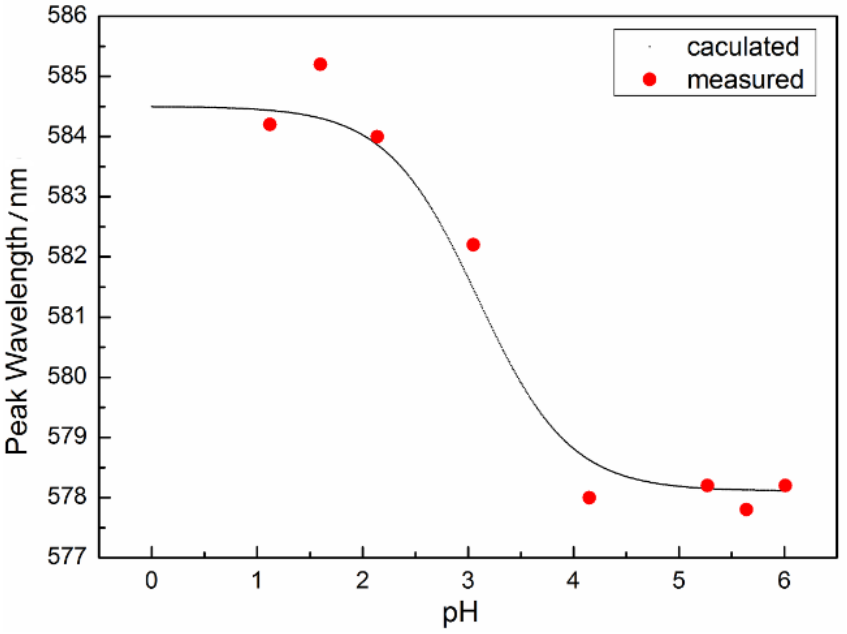


Fig. 3-5 Fluorescence peaks of RhB in bulk as a function of the bulk pH

the pKa. This is supported by an equation deriving from Eq. (3-12), Eq. (3-13) and Eq. (3-14). A pKa of 3.2 was estimated using these data, in which similar quantum yields and shapes of the fluorescence spectra between the cationic and zwitterionic forms of RhB are assumed to have the theoretical curve shown in Fig. 3-5. The pKa of 3.2 is close to the literature value of 3.1.[21]

The pH dependence of the fluorescence peak wavelengths of RhB molecules adsorbed at the air/water interface is shown in Fig. 3-6. Comparing Fig. 3-5 with Fig. 3-6, it was found that from the bulk to the air/water interface, both peak wavelengths of the $RhBH^+$ and $RhB^{\pm}$ forms show about a 2-nm red shift, or -61.2 $cm^{-1}$ and -47.7 $cm^{-1}$ in energy, respectively. The fluorescence peak wavelengths of two different RhB forms were acquired at pH values lower than 2 or higher than 4. The $RhBH^+$ form at the air/water interface had a fluorescence peak at 587 nm, while the $RhB^{\pm}$ form has one at 572 nm. Under the same assumption for bulk solution, an apparent value of $pK_{a,surf}$ was calculated to be 3.5 with these data. Although this is not the true value of $pK_{a,surf}$, it is notable that RhB had a good performance as a surface-active and fluorescent pH indicator having a certain $pK_{a,surf}$ value around 4 at the air/water interface. Such a surface-active and fluorescent pH indicator has potential for studying pH-relating chemical and physical phenomena occurring at the air/water interface under little invention of the probe molecules.

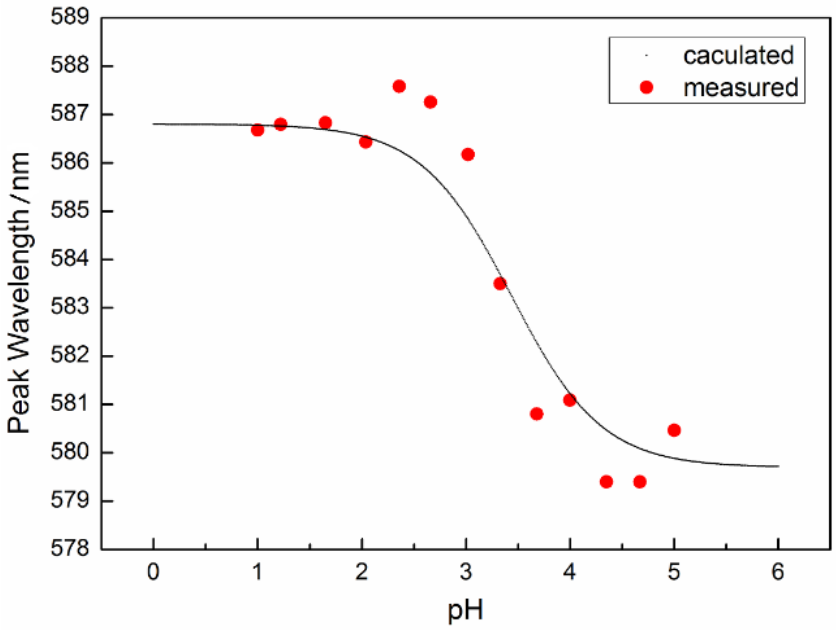


Fig. 3-6 Fluorescence peaks of RhB at the air/water interface as a function of the bulk pH

To determine the true value of $pK_{a,surf}$, evaluation of the forward and backward reaction rates of the acid-base equilibrium is straightforward when using a pH-jump method. Although the water surface-selective pH-jump method has not been established, it could be performed because the adsorption–desorption equilibrium of solute molecules at the air/water interface is expected to be a much slower process than the acid-base equilibrium.

As another way to estimate the value of $pK_{a,surf}$, the solvent effects of RhB could be utilized. Table 3-1 gives the fluorescence peak wavelengths of RhB in a variety of organic solvents. Among these measured organic solvents, $RhB^{\pm}$ in ethane-1,2-diol shows a closer extent (3 nm) of red shift to that at the air/water interface. It is considered that solute molecules adsorbed at the air/water interface are in an intermediate dielectric environment between air and water. If the dielectric constant is the dominant factor of forward and backward reaction rates of the acid-base equilibrium, $K_{a,surf}$ can be estimated by determining $K_a$ in ethane-1,2-diol. This could be another way to estimate $K_{a,surf}$.

Table 3-1 The fluorescent peaks of $RhB^{\pm}$ in a variety of solvents and at the air/water interface

| Solvent | Relative dielectric constant | Peak wavelength/nm |
|---|---|---|
| n-propanol | 20 | 569 |
| ethanol | 25 | 571 |
| ethane-1,2-diol | 39 | 581 |
| propane-1,2,3-triol | 43 | 584 |
| water | 80 | 578 |
| formamide | 110 | 608 |
| the air/water interface | - | 580 |

### 3.3.3 Surface Tension Experiments

With $pK_{a,surf}$, $\Delta_{pH}$ can be determined using Eq. (3-6) because the other values of $N_{max,RhBH^+}$, $N_{max,RhB^{\pm}}$, $K_{ad,RhBH^+}$, and $K_{ad,RhB^{\pm}}$ are determinable with surface tension measurements, as described below. Figure 3-7[25] shows the surface tension of RhB aqueous solutions at pH 1.2 and pH 5.5 as a function of the concentration. The pH 1.2 and pH 5.5 values were selected because RhB molecules exist in the $RhBH^+$ form at pH 1.2 and in the $RhB^{\pm}$ form at pH 5.5 in aqueous solutions. As the RhB concentration increases, the surface tension of the aqueous solutions shows a decreasing trend, which indicates that RhB is surface-active independent of the chemical forms. From the surface tension, the corresponding surface density is obtained using the Gibbs adsorption isotherm.[26]

$N_{max,RhBH^+}$, $N_{max,RhB^{\pm}}$, $K_{ad,RhBH^+}$, and $K_{ad,RhB^{\pm}}$ were calculated to be 0.72 μmol·m$^{-2}$, 0.64 μmol·m$^{-2}$, $2.7\times10^5$ M$^{-1}$, and $6.5\times10^5$ M$^{-1}$, respectively. With these values, the surface density of $1.0\times10^{-8}$ M RhB solution is estimated to be 1.93 nmol·m$^{-2}$ and 4.13 nmol·m$^{-2}$ under acidic

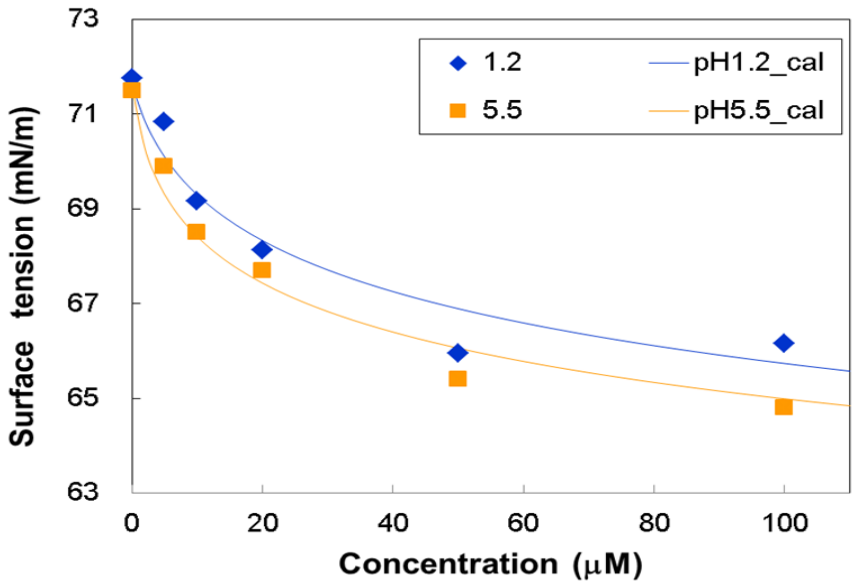


Fig. 3-7 Surface tension of RhB aqueous solutions as a function of the concentration.

and basic conditions, respectively. These densities seem to be small enough to negate the effect of probes on the pH at the air/water interface.

### 3.3.4 Basic Fluorescence pH Indicators

It is a bit reluctant to use RhB only to demonstrate this new pH-determination method, because RhB is an acid fluorescence pH indictor. From this angle, another basic fluorescence pH indicator is also required to be attempted with this new pH-determination method. However, due to limitations of our experimental conditions, there are few basic fluorescence pH indicators that can be attempted in this experiment. Three basic conditions that they have to be required, including 1) a fluorescence pH indicator with ratiometric property, 2) exciting wavelength around 532 nm, and 3) emission wavelength around 550~650 nm. Carboxy-SNARF is one of such basic fluorescence pH indicators.

Different kinds of pH buffer solution systems were tried and demonstrated, for maintaining pH according to our own interest. As shown in Tab. 3-2, by mixing 0.1 M HCl and 0.1 M sodium citrate solution in different ratios, an acid pH from 1 to 5 can be obtained according to our own interest. By mixing 0.1 M potassium dihydrogen phosphate solution and 0.1 M sodium hydrogen phosphate solution in different ratios, a basic pH from 6-9 are able to be obtained according to our own interest.

Table 3-2 different kinds of pH buffer solution systems

| 0.1 M HCl (mL) | 0.1 M $Na_2HC_6H_5O_7$ (mL) | pH | 0.1 M $KH_2PO_4$ (mL) | 0.1 M $Na_2HPO_4$ (mL) | pH |
|---|---|---|---|---|---|
| 10.00 | 0 | 1.08 | 9.00 | 1.00 | 5.87 |
| 6.67 | 3.33 | 2.29 | 3.00 | 7.00 | 7.14 |
| 5.50 | 4.50 | 3.36 | 1.00 | 9.00 | 7.70 |
| 4.00 | 6.00 | 4.19 | 0.50 | 9.50 | 8.01 |
| 0 | 10.00 | 4.90 | 0 | 10.00 | 9.02 |

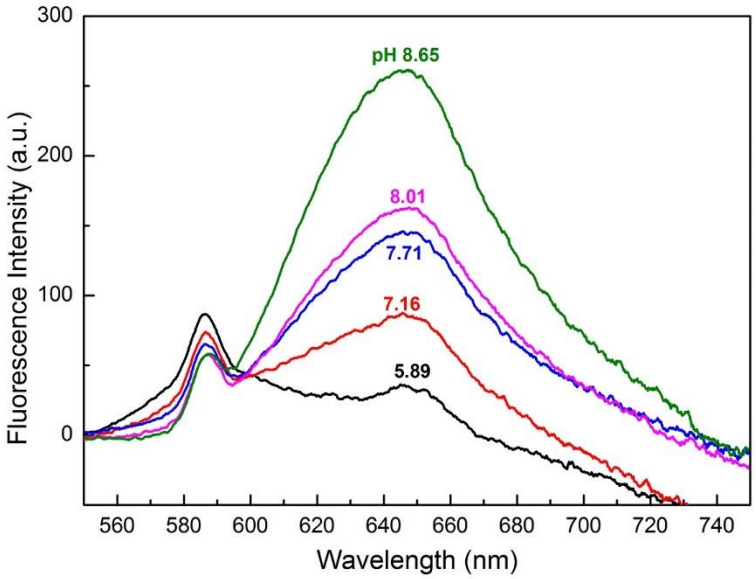


Fig. 3-8 Emission spectra of Carboxy-SNARF in different pH solutions (bulk)

5-(and-6)-carboxyseminaphthorhodafluor-1 is selected as the first basic fluorescence pH indicator for estimating the pH with this new method. SNARF is a good ratiometric fluorescence indicator that has strong pH dependence in water bulk, and with a pKa of 7.5[27]. In Fig. 3-8, under an exciting wavelength of 532 nm, as the pH increases, the fluorescence peak at 645 nm becomes taller, whereas that at 585 nm becomes shorter. As shown in Fig. 3-9, the intensity ratio of these two peaks varies with the pH 4~11. It was also confirmed that SNARF is a basic fluorescence pH indicator that largely different from RhB.

The fluorescence spectrum of RhB molecules adsorbed at the air/water interface was successfully acquired with a CFM. Figure 3-4 shows the fluorescence spectra of RhB aqueous solutions measured with different laser focus positions along the depth direction. The intensity of fluorescence was not normalized and not smoothed: these fluorescence spectra were all raw data acquired with a CFM. When the laser beam was rightly focused at the air/water interface (0 μm), a broad and strong peak at 584 nm was observed. This fluorescence spectrum was attributed to that of RhB adsorbed at the air/water interface. When

the laser beam was focused under 100, 200, and 300 μm downward from the solution surface, that strong and broad peak turned into a broad and weak peak at 579 nm.

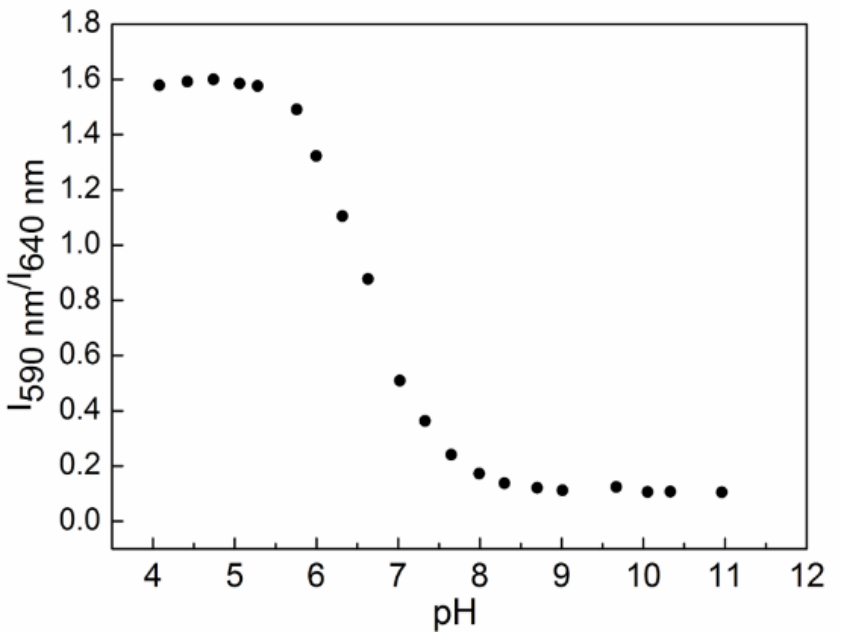


Fig. 3-9 The intensity ratio of fluorescence peak at 585 nm to that at 645 nm varies with the pH

These fluorescence spectra were attributed to that of RhB in bulk. When the laser beam was focused at 100 μm upward from the solution surface in the gas phase, almost no peak was observed.

The fluorescence spectrum of SNARF molecules adsorbed at the air/water interface was also tried to be acquired the CFM. Figure 3-10 shows fluorescence spectra of SNARF aqueous solutions measured with different laser focus positions along the depth direction, similar to those of RhB molecules shown in Fig. 3-4. However, no fluorescence spectrum of SNARF molecules adsorbed at the air/water interface was apparently observed. In fact, the fluorescence spectrum obtained at 0 μm should be attributed to fluorescence spectrum of the

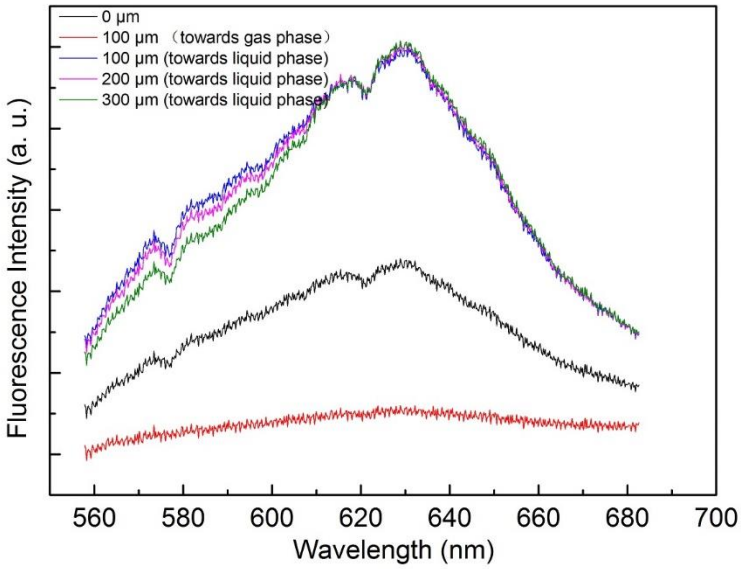


Fig. 3-10 Fluorescence spectra of SNARF aqueous solutions measured with different laser focus positions along the depth direction (pH = 9.59)

water bulk, rather than that of the air/water surface. The shape of fluorescence spectrum measured when the laser beam was rightly focused at the air/water interface (0 μm), is almost the same with those when at the laser beam was focused under 100, 200, and 300 μm downward from the solution surface, expect that the height of the former one is about half of those of the others.

The reason may be that the surface density of SNARF is so small that only fluorescence emissions from half of the probe area were collected when the laser beam was right focused at the air/water interface.[19] So it is expected that why the height of fluorescence spectrum at the air/water interface is about half of that in the water bulk.

### 3.3.5 Mathematical Relationship between Fluorescence Peak Wavenumbers and pH for a Fluorescent pH Indicator

In a CFM, the probe volume is confined in an elongated cylindrical shape with radius w and

height $2d_z$. If the position of the surface is defined to be exactly at the symmetrical plane horizontally intersecting the cylinder, the probe area and probe volume are $\pi w^2$ and $\pi w^2 d_z$ for the surface observation, while they are zero and $2\pi w^2 d_z$ for the bulk observation, respectively. For a component i, the ratio of fluorescent intensity detected for the surface observation with respect to the bulk observation can be given as

$$R_{f,i} = \left(\eta_{surf,i}\pi w^2 N_i + \eta_{bulk,i}\pi w^2 d_z C_i\right)\Big/\left(2\eta_{bulk,i}\pi w^2 d_z C_i\right) = \eta_{surf,i}N_i/2\eta_{bulk,i}d_z C_i + 1/2, \quad (3\text{-}7)$$

where $\eta_{surf,i}$ and $\eta_{bulk,i}$ represent the efficiencies of fluorescence excitation detection per fluorescent molecule at the surface and in the bulk solution, respectively; $N_i$ is the surface density, and $C_i$ is the bulk concentration. Because $N_i = N_{max,i}K_{ad,i}C_i$, Eq. (3-7) is deformed into

$$R_{f,i} = \eta_{surf,i}N_{max,i}K_{ad,i}/2\eta_{bulk,i}d_z + 1/2, \quad (3\text{-}8)$$

when $R_{f,i} \gg 1$, a surface-selective observation for this surface-active component at the water surface is available.[17]

In this case, and at a low concentration limit, the pH-dependent fluorescence spectrum of the surface-adsorbed pH indictor is given by

$$F_{surf}(\nu, pH) = \eta_D \pi w^2 I_E \left\{N_A \eta_{surf,A}(\nu) + N_B \eta_{surf,B}(\nu)\right\}, \quad (3\text{-}9)$$

where $\eta_D$ is proportionality constant for the equipment, $I_E$ is the excitation laser power, $\nu$ is the fluorescence photo frequency, A and B are acid and basic forms of the pH indicator, respectively. Here, it is assumed that fluorescent spectra of the both acid and basic forms are pH independent. At a low concentration limit, where $N_i = N_{max,i}K_{ad,i}C_i$, Eq. (3-9) is deformed into

$$F_{surf}(\nu,pH) = \eta_D \pi w^2 I_E C \left\{ N_{max,A} K_{ad,A} \alpha \eta_{surf,A}(\nu) + N_{max,B} K_{ad,B} (1-\alpha) \eta_{surf,B}(\nu) \right\}, \quad (3\text{-}10)$$

where $\alpha$ is the fraction of the acid form in the solution's surface region.

The pH-dependent fluorescent spectrum of the bulk indicator is given by

$$F_{bulk}(\nu,pH) = 2\eta_D \pi w^2 d_z I_E C \left\{ \alpha' \eta_{bulk,A}(\nu) + (1-\alpha') \eta_{bulk,B}(\nu) \right\}, \quad (3\text{-}11)$$

where $\alpha'$ is the fraction of the acid form in the solution's bulk region.

At the fluorescence maxima, we have $\partial F_x(\nu_{max}, pH)/\partial\nu = 0$ both for surface (x=surf) and bulk (x=bulk). For simplicity, the fluorescence spectrum shapes around the fluorescence maxima are assumed to be $\eta_{x,i}(\nu) = I_{x,i}\left\{1 - (\nu-\nu_{x,i})^2 / w_{x,i}^2\right\}$ (i=A, B), so that $\frac{\partial \eta_{x,i}(\nu)}{\partial \nu} = \frac{2I_{x,i}(\nu-\nu_{x,i})}{w_{x,i}^2}$, and we get

$$\nu_{max,x} = \frac{\nu_{x,A} + \nu_{x,B} g_x}{1+g_x}, \quad (3\text{-}12)$$

where

$$g_{surf} = \frac{I_{surf,B} w_{surf,A}^2}{I_{surf,A} w_{surf,B}^2} \frac{K_{a,surf} 10^{\Delta pH}}{[H^+]}, \quad (3\text{-}13)$$

and

$$g_{bulk} = \frac{I_{bulk,B} w_{bulk,A}^2}{I_{bulk,A} w_{bulk,B}^2} \frac{K_a}{[H^+]}. \quad (3\text{-}14)$$

The values of $K_{a,surf}10^{\Delta pH}$ can be determined through Eq. (3-6) after obtaining the values of $N_{max,\ RhBH^+}$, $N_{max,\ RhB^\pm}$, $K_{ad,\ RhBH^+}$, and $K_{ad,\ RhB^\pm}$ with surface tension measurements. $K_a$ is a known value. Both $\frac{I_{surf,B} w_{surf,A}^2}{I_{surf,A} w_{surf,B}^2}$ and $\frac{I_{bulk,B} w_{bulk,A}^2}{I_{bulk,A} w_{bulk,B}^2}$ are assumed to be 1.

Therefore, a mathematical relationship between fluorescence peak wavenumbers and pH is clearly understood through Eq. (3-12), Eq. (3-13), and Eq. (3-14).

## 3.4 Conclusion

A method to determine pH at the air/water interface with a confocal fluorescence microscope was proposed. A relationship between the pH at the air /water interface and that in bulk solution was formulated in connection with the adsorption equilibrium and dissociation equilibrium of the dye adsorbed. RhB was used as an acid fluorescent pH probe in this research. The corrected fluorescence spectrum of RhB molecules at the air/water interface with the surface density of 1.0 $nmol \cdot m^{-2}$ level showed pH-dependent shifts representing an acid-base equilibrium. Two ways to determine the unknown property, $pK_{a,surf}$ of RhB molecules at the air/water interface were discussed. With surface-tension measurements, the adsorption properties, the maximum surface density, and the adsorption equilibrium constants were estimated for both cationic and zwitterionic forms of RhB molecules at the air/water interface. SNARF, as a basic fluorescence pH indicator, was also tried to be applied with this method, and some preliminary results were obtained. Considering the advantages of the fluorescence method, such as high sensitivity, this work provides new insight and inspiration for studying the water surface's acidity.

## References


1. A. Harata, M. Sato, and T. Ishioka, *"Charged Particle and Photon Interactions with Matter: Recent Advances, Applications, and Interfaces"*, ed. Y. Hatano, Y. Katsumura, and A. Mozumder, **2010,** CRC press, Boca Raton, 445.
2. S. Yamaguchi, K. Bhattacharyya, and T. Tahara, *J. Phys. Chem. C,* **2011**, *115*, 4168.
3. Y. Kazoe, K. Mawatari, Y. Sugii, and T. Kitamori, *Anal. Chem.,* **2011**, *83*, 8152.
4. V. Buch, A. Milet, R. Vacha, P. Jungwirth, and J. P. Devlin, *Proc. Natl. Acad. Sci. U.S.A.,* **2007,** *104,* 7342.
5. Y. Tabe, N. Kikkawa, H. Takahashi, and A. Morita, *J. Phys. Chem. C,* **2014,** *118,* 977.
6. M. Takahashi, *J. Phys. Chem. B,* **2005,** *109,* 21858.
7. A. S. Najafi, J. Drelich, A. Yeung, Z. H. Xu, and J. Masliyah, *J. Colloid Interface Sci.,* **2007,** *308,* 344.
8. S. Enami, M. R. Hoffmann, and A. J. Colussi, *J. Phys. Chem. Lett.,* **2010,** *1,* 1599.
9. X.-L. Zhao, S.-W. Ong, H.-F. Wang, and K. Eisenthal, *Chem. Phys. Lett.,* **1993,** *214*, 203.
10. P. B. Petersen and R. J. Saykally, *J. Phys. Chem. B,* **2005,** *109,* 7976.
11. P. B. Petersen and R. J. Saykally, *Chem. Phys. Lett.,* **2008,** *458,* 255.
12. T. L. Tarbulk, S. T. Ota, and G. L. Richmond, *J. Am. Chem. Soc.,* **2006,** *128,* 14519.
13. M. Mucha, T. Frigato, L. M. Levering, H. C. Allen, D. J. Tobias, L. X. Dang, and P. Jungwirth, *J. Phys. Chem. B,* **2005,** *109,* 7617.
14. C.-S. Tian, N. Ji, G. A. Waychunas, and Y. R. Shen, *J. Am. Chem. Soc.,* **2008,** *130,* 13033.
15. S. Yamaguchi, A. Kundu, P. Sen, and T. Tahara, *J. Chem. Phys.,* **2012,** *137,* 151101.
16. M. Sato, A. Harata, Y. Hatano, T. Oagawa, T. Kaieda, K. Ohmukai, and H. Kawazumi, *J. Phys. Chem. B*, **2004,** *108,* 12111.
17. Y.-Q. Li, M. N. Slyadnev, T. Inoue, A. Harata, and T. Ogawa, *Langmuir,* **1999,** *15,* 3035.
18. Y.-Q. Li, T. Inoue, A. Harata, and T. Ogawa, *Instrum Sci. Technol.,* **1999,** *27,* 159.
19. X.-Y. Zheng, A. Harata, and T. Ogawa, *Specrtochim. Acta, Part A,* **2001,** *57,* 315.
20. J.-Y. Han and K. Burgess, *Chem. Rev.,* **2010,** *110,* 2709.
21. I. L. Arbeloa, *Chem. Phys. Lett.,* **1986,** *128,* 474.
22. H.-J. Butt, K. Graf, and M. Kappl, *"Physics and Chemistry of Interfaces"*, **2006,** Wiley-

VCH Verlag GmbH & Co. KGaA, Weinheim.

23. L. X. Dang and T.-M. Chang, *J. Chem. Phys.,* **1997,** *106,* 8149.

24. E. A. Raymond, T. L. Tarbuck, M. G. Brown, and G. L. Richmond, *J. Phys. Chem. B,* **2003,** *107,* 546.

25. Y. Imanishi, "*Development of a pH-determination Method at the Air/water Interface with a Confocal Fluorescence Microscope*", **2012**, unpublished master thesis, Kyushu University.

26. A. J. Prosser and E. I. Franses, *Colloids Surf., A,* **2001**, *178,* 1.

27. J. E. Whitaker *et al*, *Anal Biochem.,* **1991**, *194*, 330.

# CHAPTER 4 Observing Excitation Spectra of Soluble Molecules Adsorbed at Air/Water Interface with a Semi-Confocal Fluorescence Microscope

## 4.1 Introduction

It is greatly important to understand the air/water interface in physical, analytical, and environmental chemistry.[1] One of topics is to study physical and chemical properties of molecules such as surfactants and water-soluble solutes adsorbed at the air/water interface.[2] Although computer-based calculation gives a large progress for molecular view of the interface recently, some difficulties make experimental approaches still uneasy, especially in observing solute molecules adsorbed at the air/water interface highly sensitively and interface-selectively. Confocal fluorescence microscope (CFM) has been applied to observe fluorescence emission of water-soluble rhodamine dyes adsorbed at the air/water interface even under the surface density of solute molecules being 1-$10^3$ molecule/$\mu m^2$.[3-5] However, it is still difficult to surface-selectively observe absorption spectra of water-soluble solute molecules adsorbed at the air/water interface, especially for aromatic hydrocarbons having no visible light-absorption. Combining with its corresponding fluorescence emission spectra, absorption spectra of molecules reveal physical and chemical properties of the air/water interface, when the air/water interface is considered as a common organic solvent.[6] Even if it is hard to observe absorption spectra directly for the solute molecules adsorbed at the air/water interface mainly because of lacks in detection sensitivity, fluorescence excitation spectra could be measured in behalf of absorption spectra.

Poly-aromatic cyclic hydrocarbons (PAHs) are ubiquitous in our atmosphere, toxic to our environment, and absorb UV light.[7] Pyrene of the target molecule in this research is one of the typical PAHs and has no visible light-absorption as is the most of environmentally important PAHs with a small molecular weight. When a conventional CFM is applied to observe the fluorescence excitation spectra of the target, there arise some difficulties: excitation wavelength in deep UV forces to use a microscopic objectives with low

transmission performance and a pulsed excitation laser with low wavelength-tunable performance in UV. These difficulties are so common in observing environmentally toxic molecules because these molecules generally have little visible light-absorption. Therefore, a new type of fluorescence microscope is counted on observing excitation spectra of PAHs molecules adsorbed at the air/water interface.

In this work, a semi-confocal fluorescence microscope (ScFM) is designed and constructed for aiming to observe fluorescence excitation spectra of soluble molecules adsorbed at the air/water interface. A total internal reflection illumination with a light-guide coupled monochromated-xenon lamp is combined with the confocal fluorescence microscope. Performance of the ScFM is evaluated and discussed. The emission characteristics of the excitation light is examined. A preliminary result about emission spectrum of pyrene molecules adsorbed at the air/water interface is obtained with this microscope.

## 4.2 Experimental

### 4.2.1 Apparatus

The experimental setup of ScFM is shown in Fig. 4-1 and Fig. 4-2, which is similar to that of CFM in our past work,[3] except for an additional incoherent UV excitation beam. Adjusting optical paths in ScFM is also completed by referring to that in CFM. A beam of polychromatic UV light emitted from a xenon lamp (Max-303UV, Asahi Spectra Co.,Ltd.) is dispersed by a monochromator (CT-10, Jasco Corp.) installing a grating with a 600 grooves/mm ruling and a blazing wavelength of 300 nm, into monochromatic UV light with a tunable wavelength from 260 nm to 400 nm. This monochromator is connected with a light guide (Quartz Light Guide, Asahi Spectra Co.,Ltd.) by means of a light guide connecter (CMS100-F.SØ20, Asahi Spectra Co.,Ltd.). The light guide transmits this tunable monochromatic UV light from the monochromator into a collimator lens (RLQL80-1, Asahi Spectra Co.,Ltd.), which clamped by an extension clamp in an iron support. The tunable monochromatic UV light emitted from the collimator lens illuminates at the interface of $1\times10^{-8}$ M pyrene aqueous solution (thickness, 2 mm) in a total internal reflection geometry. Pyrene solution is loaded in a quartz cell (40 mm × 40 mm × 20 mm). Fluorescence emissions generated at the air/water interface are collected with fluorescence collection system made up of an objective lens (UPLFLN40C, Olympus), a lens (SLSQ-20-50p, Sigma Koki) and a pinhole (diameter, 200 μm). The only focus point of this microscope is existing in this fluorescence collection system, different from CFM that also has another focus point existing in illuminating the sample with laser. So we call it a semi-confocal fluorescence microscope. A polychromatic spectroscope (PMA-100, Hamamatsu; 300 grooves/mm, 600 nm) receives fluorescence emissions and complete photoelectric conversion with an image intensifier unit and a charge coupled device inside, under experimental conditions of exit slit of 10 μm, entrance slit of 100 μm, and accumulation time of 20 s. An electricity-based cooling system is induced to keep temperature of the charge coupled device at -14.5 ℃ to reduce noise. A personal computer records and analyzes fluorescence signals with its software (U8167-02, Ver 1.3.0). Although fluorescence emissions generated in bulk are collected simultaneously, their intensity are reasonable to be reduced substantially, and thus a surface-selective

collection is achieved.

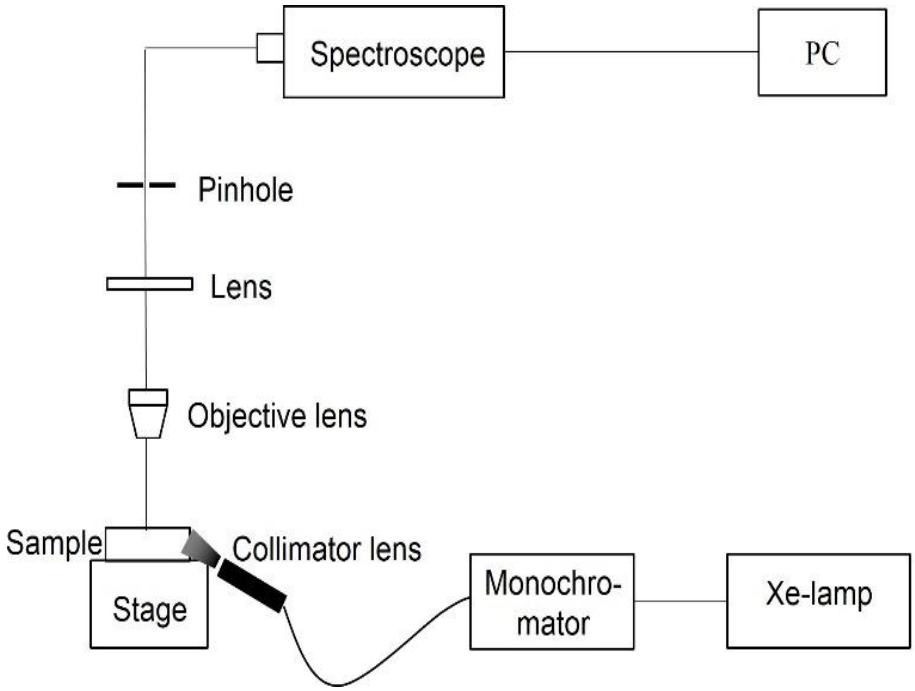


Fig. 4-1 The schematic illustration of the semi-confocal fluorescence microscope

Each part of the ScFM this microscope was checked of the wavelength range, wavelength accuracy, and spectral resolution to qualify the spectroscope, especially for measuring fluorescence emission spectra and of PAHs. The emission wavelength axis was calibrated with three main spectral lines of 365.015 nm, 404.656 nm and 435.833 nm of a mercury lamp (L937-01, Hamamatsu). The resolution of the spectroscope in UV region is evaluated to 1 nm of the full width at full width at half maximum (FWHM) for the 365.015 nm spectral line of mercury lamp.

For optimization of entrance slit and exit slit in the monochromator connected to the light source, the central wavelength of the light source was set at 357 nm. For obtain an optimal entrance slit, the entrance slit was varied from 0.10 mm to 0.36 mm while exit slit was maintained at 0.31 nm; For obtaining an optimal exit slit, the entrance slit was varied from 0.25 mm to 0.35 mm while entrance silt was maintained at 0.36 nm. The light intensity of

the light source is constantly set at 100%.

For the fluorescence spectra of pyrene solution measured under different z-axis positions, the concentration of pyrene solution is about $1.0 \times 10^{-6}$ mol/L. The exciting light is a beam of polychromatic light with a wavelength range between 310-360 nm emitting from the light source. When the lamp beam was focused on the air/water interface, it was considered as 0 μm. And moving towards gas phase was considered positive, The fluorescence spectra of pyrene solution under 200 μm, 500 μm, -200 μm, -500 μm, -1000 μm, and -2000 μm were all acquired. All of the experiments described above were performed at room temperature.

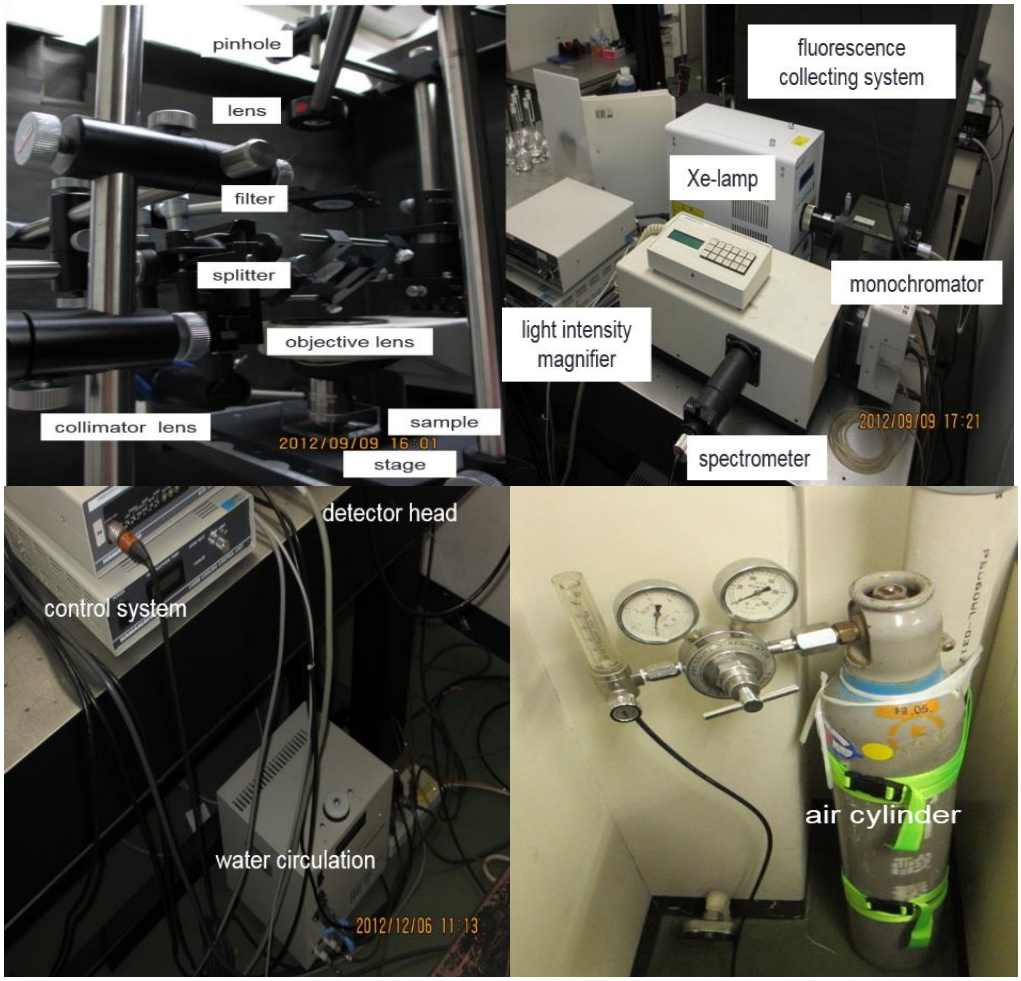


Fig. 4-2 The photographic illustration of the semi-confocal fluorescence microscope

### 4.2.2 Chemicals

Pyrene was selected as one typical example of PAHs. $1\times10^{-8}$ M pyene aqueous solution was used as sample solution. Pyrene (purity, 99%) was purchased from Janssen Chimica (Beerse, Belgium). Water was purified with water purification system (Milli-Q Academic A10, Millipore). $1\times10^{-6}$ M pyrene aqueous solution was acquired directly from pyrene's saturated solution, and $1\times10^{-8}$ M pyrene aqueous solution was acquired by diluting that of $1\times10^{-6}$ M pyrene aqueous solution.

## 4.3 Results and Discussion

### 4.3.1 Excitation Light Source

A tunable monochromatic and UV light emitted from the light guide connected from the monochromator and the xenon lamp was assessed with the corrected spectroscope of ScFM. As shown in Fig. 4-3, the monochromatic light with a wavelength range of 260 nm to 400 nm are obtained: each emission spectrum of the light source is collected respectively under the condition of the CT-10 monochromator being set at 130.0 nm, 140.0 nm, 150.0 nm, 160.0 nm, 170.0 nm, 180.0 nm, 190.0 nm, or 200.0 nm. This wavelength range fully covers absorption maxima of pyrene as well as a variety of PAHs.

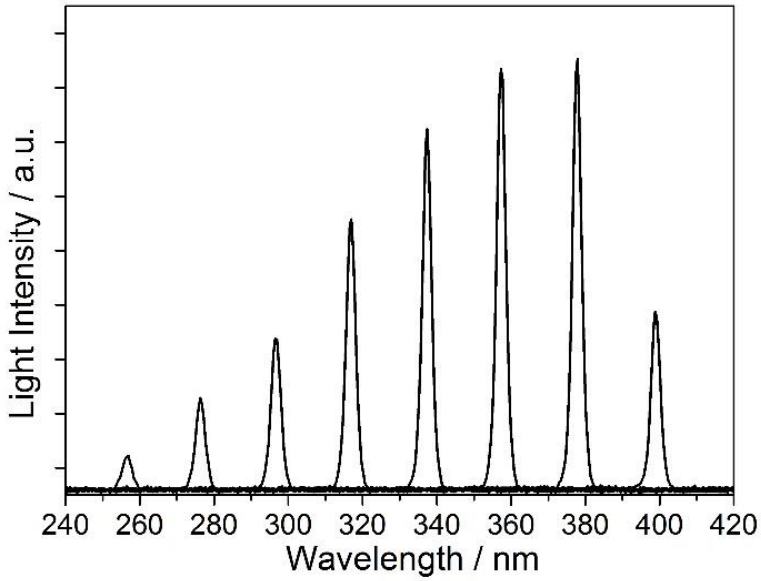


Fig. 4-3 The monochromatic light with a wavelength range of 260 to 400 nm obtained with the excitation light source

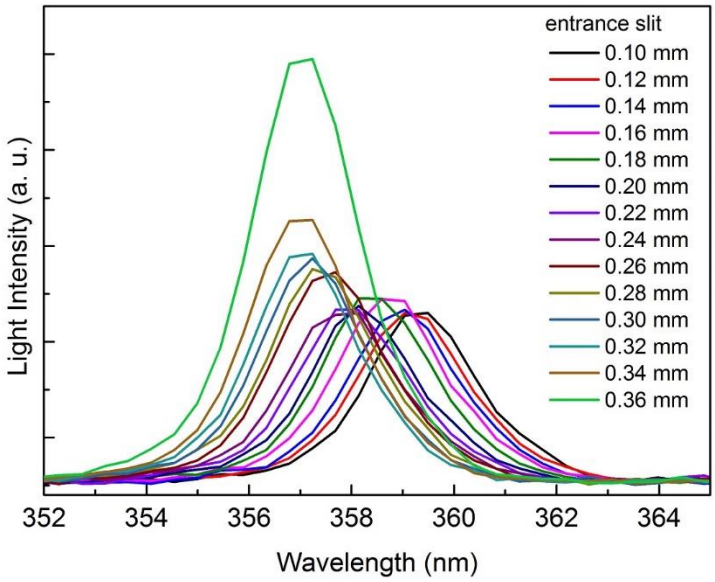


Fig. 4-4 Optimization of entrance slit in the monochromator connected to the light source

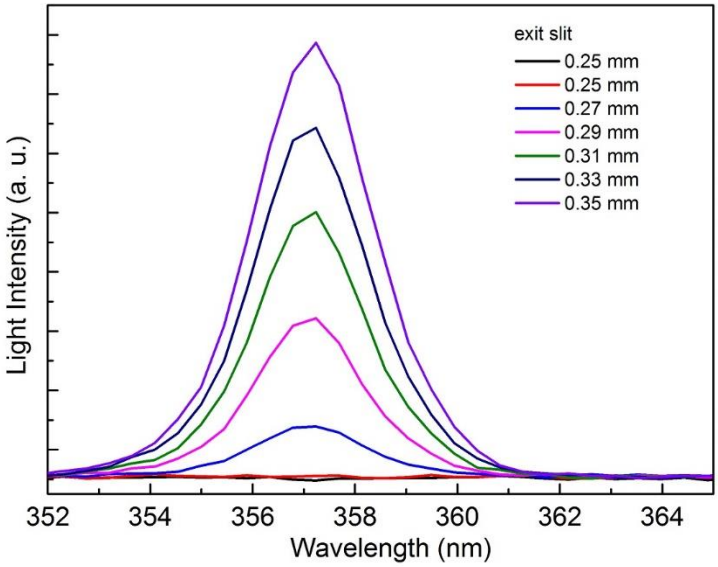


Fig. 4-5 Optimization of exit slit in the monochromator connected to the light source

The entrance slit and exit slit in the monochromator connected to the light source was optimized with the purpose of ensuring the highest resolution. The result is shown in Fig. 4-4 and 4-5. The optimal entrance slit and exit slit are 0.32 mm and 0.27 mm, respectively. For the width of entrance slit and exit slit thinner than those optimal values, the initial peak wavelength of emitting light at 357 nm have an obvious and large blue shit (Fig. 4-4), or the initial peak wavelength of emitting light at 357 nm were diminished into a flat line due to a lack of light (Fig. 4-5).

The monochromaticity of UV light emitted from xenon lamp and monochromator was investigated. The spectrum of the monochromatic light at 357 nm is shown in Fig. 4-6. Its monochromaticity was optimized by checking the dependence on the widths of the entrance and exit slits: i. e., for the monochromatic light at 357 nm, the best resolution was obtained with the entrance and exit slit widths of 0.32 mm and 0.27 mm, respectively. The FWHM of this UV monochromatic light is calculated to be 2.0 nm, higher than 13 nm[8] and 5 nm[9] of

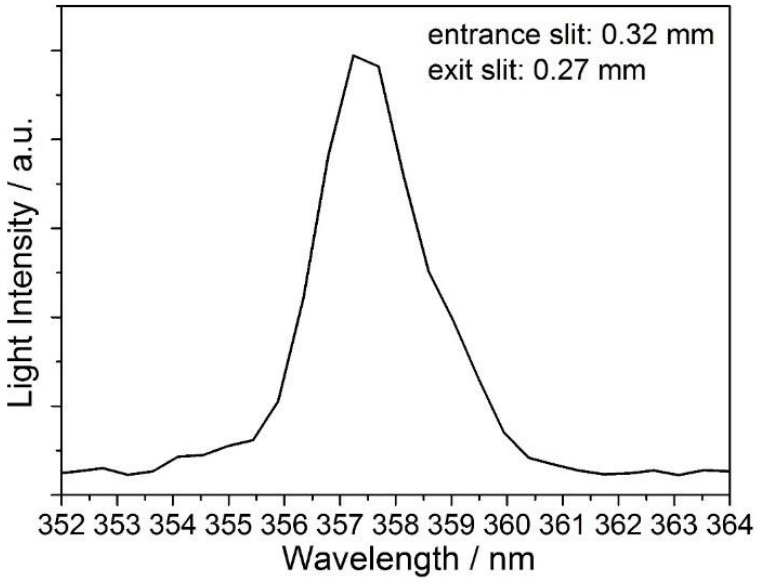


Fig. 4-6 The monochromatic light of 357 nm emitted from the xenon lamp and the monochromator

other reported ones. This level of monochromaticity is enough to discuss dependence of the Stokes' shift on environment molecules feel.[6] At 300 nm, 2 nm red shift corresponds to 220 $cm^{-1}$ shift which is smaller than the typical values of Stokes' shift. The results show that the light source in ScFM developed can provide monochromatic UV light with 2.0 nm FWHM in the wavelength range between 260 nm and 400 nm. In conclusion, the light source is successfully obtained for observing excitation spectra of PAHs adsorbed at the air/water interface with ScFM.

### 4.3.2 Fluorescence Spectrum of Pyrene Molecules Adsorbed at the Air/Water Interface

It is generally expected that ScFM has no good surface-selectivity in observing fluorescence emission: fluorescence both from bulk solution and from surface is detected, and the contribution ratio $R_f$ of surface depends on surface activity of the target molecules and on thickness of the liquid solution, as shown in Eq. (4-1),[5] except for the fact that $d_z$ represents the solution thickness instead of the height of the probe volume.

$$R_f = (\eta_s \pi \omega^2 N_s + \eta_b \pi \omega^2 d_z C)/(2\eta_b \pi \omega^2 d_z C) = \eta_s N_s / 2\eta_b d_z C + 1/2 \qquad (4\text{-}1)$$

Where $\eta_s$ and $\eta_b$ are the efficiencies of fluorescence excitation-detection for fluorescence molecules at the air/water interface and in water bulk. $\omega$ is the radius of the cylinder-shaped probe volume of ScFM. $N_s$ is the surface density of targeted molecules. $C$ is the bulk concentration of target molecules.

Since $N_s = KN_{max}C$, where $K$ is the adsorption equilibrium constant, and $N_{max}$ is the maximum surface density of target molecules, Eq. (4-1) can be deformed into,[5]

$$R_f = \eta_s K N_{max} / 2\eta_b d_z + 1/2 \qquad (4\text{-}2)$$

As shown in Eq. (4-2), it is simply expected that surface-selective observation is possible for target molecules with a high surface activity represented by $K$ or $N_{max}$ and a small solution

thickness $d_z$.

Figure 4-7 shows the fluorescence spectrum of pyrene molecules in the bulk solution measured with ScFM, excited by a band of mixed excitation light with a wavelength range between 310 nm and 360 nm from the excitation light source. This fluorescence spectrum was acquired under the experimental conditions of a large solution thickness of about 15 mm and the focus of objective lens into the water bulk. It is clear that this microscope can be used to observe fluorescence of PAHs.

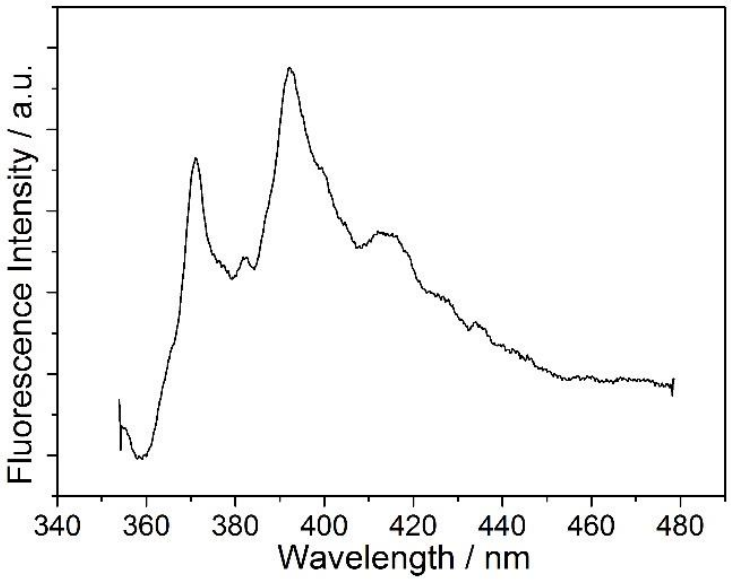


Fig. 4-7 The fluorescence spectrum of pyrene molecules in water bulk measured with the semi-confocal fluorescence microscope

Figure 4-8 shows fluorescence spectra of pyrene molecules measured with ScFM under three different positions of the objective lens focusing. The position of 0 μm means that the focus of the objective lens is just at the water surface.

There was no significant position-dependence of fluorescence intensity as shown in Fig. 4-8. In order to distinguish fluorescence emissions of pyrene molecules adsorbed at the air/water

interface from those in bulk, the ratio of fluorescence intensity at 391.1 nm with respect to that at 370.6 nm (Ⅲ/ Ⅰ ratio) are calculated and summarized in Table 4-1. This Ⅲ/ Ⅰ ratio is known to take 0.64 for pyrene in aqueous solution and 0.74 for pyrene adsorbed at the air/water interface.[10] The Ⅲ/ Ⅰ ratios in Tab. 1 are quite different from the reported ones, because they are uncorrected emission spectrum. However, the Ⅲ/ Ⅰ ratios in Tab. 1 still do not affect us to conclude that these three fluorescence spectra of pyrene measured with ScFM are all dominated by pyrene molecules in the bulk solution. Although the thickness of pyrene solution is only 2 mm, the intensity of fluorescence emissions of pyrene molecules in bulk was so high that it covers those adsorbed at the water surface. It is concluded that pyrene has a weak surface activity for observing fluorescence surface-selectively with ScFM developed.

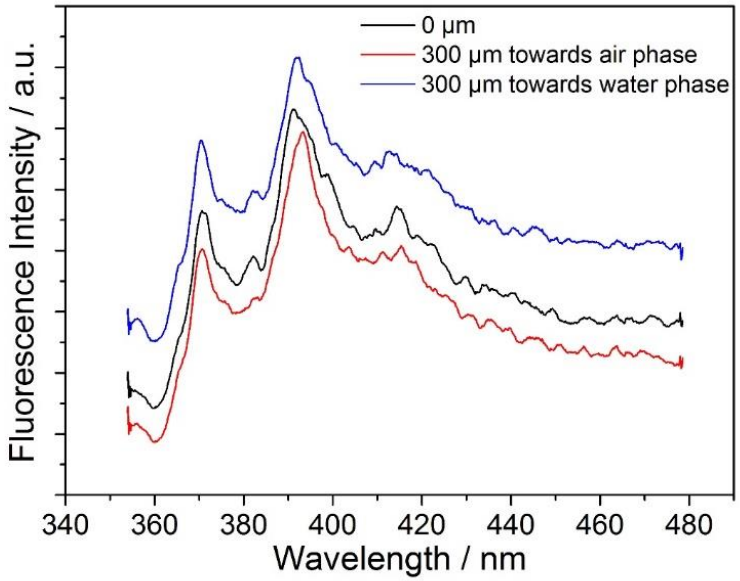


Fig. 4-8 Fluorescence spectra of pyrene molecules measured with the semi-confocal fluorescence microscope under different objective lens focusing positions

The z-axis resolution for this semi-confocal fluorescence microscope was also estimated. Figure 4-9 shows the fluorescence spectra of pyrene solution measured under different z-axis positions. As the focus point of the lamp beam moves upward and downward in different

distances, respectively, neither the fluorescence intensity nor the shape of the fluorescence spectrum of pyrene molecules at 0 μm has a significant change, expect that the fluorescence intensity of pyrene solution decreased slightly when the lamp beam focused on -2000 μm. The reason may be that the probe volume was decreased when the focus point of the lamp beam moving from 0 μm to -2000 μm.

Tab. 4-1 Ⅲ/ Ⅰ ratios of fluorescence spectra of pyrene molecules measured with semi-confocal fluorescence microscope

| | Ⅲ/ Ⅰ ratio |
|---|---|
| bulk | 1.024 |
| 0 μm | 1.024 |
| 300 μm (towards air phase) | 1.020 |
| 300 μm (towards water phase ) | 1.017 |

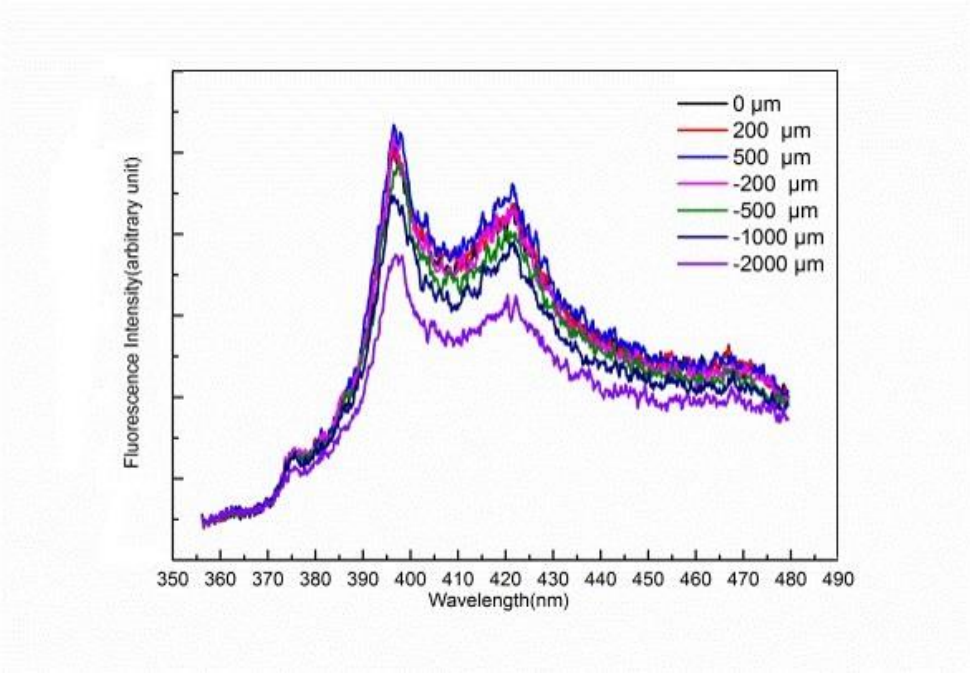


Fig. 4-9 The fluorescence spectra of pyrene solution measured under different z-axis positions

## 4.4 Conclusion

A semi-confocal fluorescence microscope is designed and constructed for observing fluorescence excitation spectrum of soluble molecules adsorbed at the air/water interface. A total internal reflection illumination of tunable monochromatic UV light from a xenon lamp is combined with a CFM. The range of wavelength and monochromaticity of the excitation light souse are examined. It can successfully provide monochromatic UV light with 2.0 nm FWHM in the wavelength range between 260 nm and 400 nm. Theoretical feasibility is discussed to obtain fluorescence spectrum of molecules adsorbed at the air/water interface surface-selectively with the microscope. The fluorescence spectra of PAHs are observed with this microscope. It is found that pyrene has a weak surface activity for observing fluorescence surface-selectively with ScFM developed.

## References


1. A. Harata, M. Sato, T. Ishioka, in *Charged Particle and Photon Interactions with Matter: Recent Advances, Applications, and Interfaces,* eds. by Y. Hatano, Y. Katsumura, A. Mozumder, CRC press, Boca Raton, **2010,** 445.
2. G. L. Richmond, *Chem. Rev.*, **2002**, *102*, 2693.
3. Y. Li, *Langmuir*, **1999**, *15*, 3035.
4. Y. Li, T. Inoue, A. Harata, and T. Ogawa, *Instrum. Sci. and Tech.*, **1999**, *27*, 159.
5. X. Zheng, A. Harata, and T. Ogawa, *Specrtochim. Acta, Part A*, **2001**, *57*, 315.
6. M. N. Slyadnev, T. Inoue, A. Harata, T. Ogawa, *Colloids Surf., A*, **2000**, *164*, 155.
7. J. Chen, F. S. Ehrenhauser, K. T. Valsaraj, and M. J. Wornat, *J. Phys. Chem. A*, **2006**, *110*, 9161.
8. K. Hirose, H. Sugahara, and H. Matsuno, *J. Light & Vis. Env.*, **2012**, *26*, 35.
9. R. J. Carman, D. M. Kane, and B. K. Ward, *J. Phys. D: Appl. Phys.*, **2010**, *43*, 025205.
10. T. Mmereki, D. J. Donaldson, *Phys. Chem. Chem. Phys.*, **2002**, *4*, 4186.

# CHAPTER 5 Conclusions and Prospects

## 5.1 Conclusions

The air/water interface is a universal but unique region, which attract great interests of researchers in recent years. Understanding the air/water interface has great importance in physical, analytical, and environmental chemistry. In this dissertation, physical and chemical properties of the air/water interface are studied by with a confocal fluorescence microscope (CFM). Based on research work of our predecessors, three original and vital research objectives are proposed: 1) to develop a CFM equipment in order to obtain a complete and corrected fluorescence spectra of soluble molecules at the air/water interface; 2) to develop a new method for determining pH at the air/water interface; 3) to develop a new type of CFM, semi-confocal fluorescence microscope, for utilizing wavelength-tunable excitation in an UV region and for observing excitation spectra of soluble molecules adsorbed at the air/water interface.

Against these three research objectives, by observing excitation and emission spectra of adsorbed soluble molecules with a CFM and a ScFM, and comparing them with those in bulk water, we developed three original chapters of research and arrived at three different conclusions.

In Chapter 2, it was concluded that a complete and corrected fluorescence spectrum of RhB molecules adsorbed at the air/water interface is obtained with the CFM developed. An updated alignment way of the CFM to acquire such a fluorescence spectrum at the air/water interface is also introduced. A certain number of basic parameters of the CFM are also obtained, including the time dependency of fluorescence density in the CFM, the solution concentration dependence of fluorescence intensity in the CFM, the depth resolution for the CFM, and the optimal smoothing orders, which helps us to know the instrument of the CFM more and better, and provide great guidance for our future research.

In Chapter 3, it was concluded that a highly sensitive method for estimating pH at the

air/water interface based on two pH-dependent dyes and the CFM was first proposed. A relationship between the pH at the air/water interface and that in bulk solution was formulated in connection with the adsorption equilibrium and dissociation equilibrium of the dye adsorbed. For determining the unknown property $pK_{a,surf}$ of RhB molecules at the air/water interface, two ways are pointed out. The adsorption properties, the maximum surface density, and the adsorption equilibrium constants were also estimated for both cationic and zwitterionic forms of RhB molecules at the air/water interface, with surface-tension measurements. As the basic fluorescence pH indicator, SNARF was also tried to be applied with this method, and some preliminary results were also obtained. Owing to high sensitivity of this new method, this work provides new insight and inspiration for studying the water surface's acidity.

In Chapter 4, in order to observe fluorescence excitation spectra of soluble molecules adsorbed at the air/water interface, a ScFM is designed and constructed. This microscope is based on a total internal reflection illumination of tunable monochromatic UV light from a xenon lamp and a CFM. It is theoretical feasible to obtain fluorescence spectrum of soluble molecules adsorbed at the air/water interface surface-selectively with this microscope. The fluorescence spectra of pyrene molecules are also observed with this microscope. It is found that pyrene has a weak surface activity for observing fluorescence surface-selectively with the developed ScFM. All conclusions in these three chapters will significantly contribute to understanding the physical and chemical properties of the air/water interface.

## 5.2 Prospects

The instrumentation of the CFM needs more and better improvement. The current optical path adjustment for focusing is mainly depended on manual operation. However, this manual operation is time-consuming and labor-consuming. It costs 30 minutes in average when we align the CFM each time. This instrument also needs extra optical path adjustment at set intervals, because the liquid level of a sample solution is often inclined to drop down ceaselessly, due to evaporation of water. Something like auto-focus mechanism are required for the sample stage. Another defect is the light source in the CFM seriously limits its application range. Although the UV lamp is lead into the microscope, it still cannot be compared with lasers, especially on the aspects of monochromaticity and brightness. Some other light sources, like UV lasers, can also be tried to be induced into this instrument, for expanding its application range and advancing some other performance.

Regarding the new method of determining pH at the air/water interface, the $pK_{a,surf}$ of RhB, as indispensable factor for obtaining the $pH_{surf}$, is an exceedingly essential question in the following research that still have not been answered. The $pH_{surf}$ value is the final result of this new method, no matter it is more acid or basic than that in the water bulk. For evaluating this newly proposed method, the obtained result of $pH_{surf}$ should be compared with those reported in the literature. Moreover, more other kinds of fluorescence pH probes, especially for basic ones, with more experimental results and conclusions, are encouraged to verify this new method of estimating pH at the air/water interface with a CFM. With more and better improvements of the instrumentation of the CFM, some other physical and chemical properties of the air/water interface besides the pH are also possible to be studied with this microscope.

Concerning the ScFM, the most essential question in the following research is to observe fluorescence spectrum of pyrene molecules at the air/water interface surface-selectively with this microscope. Even with a highly sensitive spectrometer in the ScFM, the light intensity of the UV lamp is too weak to excite more pyrene molecules to give out fluorescence

emissions with strong enough intensity. After obtaining the fluorescence spectrum of pyrene molecules at the air/water interface surface-selectively, the fluorescence excitation spectra of pyrene molecules are also able to be obtained, by shifting different excitation wavelengths and obtaining the fluorescence spectra of pyrene molecules at the air/water interface under different excitation wavelengths. By combining the fluorescence spectra and excitation spectra of more soluble molecules at the air/water interface, some certain physical and chemical properties of the air/water interface tends to be deduced.

# List of Publications and Presentations

## Publications

1. Haiya Yang, Yasushi Imanishi, Akira Harata, *Anal. Sci.,* **2015**, *31(10)*, 1005-1010.
2. Haiya Yang, Akira Harata, *Evergreen*, **2015,** *2(2)*, 1-4.

## Presentations

1. Haiya Yang, Akira Harata, "*Design of a Semi-confocal Fluorescence Microscope for Observing Surface-selective Excitation Spectra of Soluble Molecules Adsorbed at the Air/water Interface*", S4P16-54, The 14th Conference of International Association of Colloid and Interface Scientists, May 16th 2012, Sendai.
2. Haiya Yang, Akira Harata, "*Design of a Semi-confocal Fluorescence Microscope for Observing Surface-select Excitation Spectra of Soluble Molecules Adsorbed at the Air/water Interface*", 3_2.050, 4_外.002, The 49th Kyushu Region Meeting on Chemistry, June 30th 2012, Kitakyushu.
3. Haiya Yang, Akira Harata, *"A New Approach of pH-Determination at the Air/water Interface with Confocal Fluorescence Microscope",* 2PG01, The 33rd International Conference on Solution Chemistry, July 9th 2013, Kyoto.
4. Haiya Yang, Yasushi Imanishi, Toshio. Ishioka, Akira Harata, "*Determination of the water surface pH using confocal fluorescence microscope*", P3017, The 62rd Annual Meeting of the Japan Society for Analytical Chemistry, Sep 12th 2013, Osaka.
5. Haiya Yang, Akira Harata, "*A Semi-confocal Fluorescence Microscope for Observing the Excitation Spectra of Soluble Molecules at the Water Surface*", PC16, The 15th Beijing Conference and Exhibition on Instrumental Analysis, Sep 25th 2013, Beijing.

# Appendix

## Correction Factors for the Spectroscope in the CFM under Pixel Positions between 80-120

| | | | | | |
|---|---|---|---|---|---|
| 547 | 0.0000 | 552 | 0.8804 | 557 | 0.9996 |
| 547.2 | 1.2728 | 552.2 | 0.8760 | 557.2 | 1.0088 |
| 547.4 | 1.1521 | 552.4 | 0.8702 | 557.4 | 1.0152 |
| 547.6 | 0.8030 | 552.6 | 0.8333 | 557.6 | 1.0420 |
| 547.8 | 0.8350 | 552.8 | 0.8145 | 557.8 | 1.0548 |
| 548 | 0.9640 | 553 | 0.8415 | 558 | 1.0257 |
| 548.2 | 1.0959 | 553.2 | 0.8629 | 558.2 | 1.0021 |
| 548.4 | 1.0903 | 553.4 | 0.9037 | 558.4 | 1.0149 |
| 548.6 | 0.9142 | 553.6 | 0.8557 | 558.6 | 1.0006 |
| 548.8 | 0.9508 | 553.8 | 0.8528 | 558.8 | 0.9867 |
| 549 | 0.9870 | 554 | 0.8421 | 559 | 0.9770 |
| 549.2 | 1.0584 | 554.2 | 0.8481 | 559.2 | 0.9547 |
| 549.4 | 1.0603 | 554.4 | 0.8680 | 559.4 | 0.9715 |
| 549.6 | 0.9903 | 554.6 | 0.8449 | 559.6 | 0.9666 |
| 549.8 | 0.9681 | 554.8 | 0.8424 | 559.8 | 0.9501 |
| 550 | 0.8791 | 555 | 0.8473 | 560 | 0.9328 |
| 550.2 | 0.8279 | 555.2 | 0.8852 | 560.2 | 0.9313 |
| 550.4 | 0.7825 | 555.4 | 0.9375 | 560.4 | 0.9391 |
| 550.6 | 0.8032 | 555.6 | 0.9462 | 560.6 | 0.9308 |
| 550.8 | 0.8064 | 555.8 | 0.9705 | 560.8 | 0.9332 |
| 551 | 0.8732 | 556 | 0.9534 | 561 | 0.9218 |
| 551.2 | 0.8564 | 556.2 | 0.9909 | 561.2 | 0.9147 |
| 551.4 | 0.8524 | 556.4 | 1.0263 | 561.4 | 0.9147 |
| 551.6 | 0.8492 | 556.6 | 1.0200 | 561.6 | 0.9247 |
| 551.8 | 0.8277 | 556.8 | 1.0204 | 561.8 | 0.9258 |

| | | | | | |
|---|---|---|---|---|---|
| 562 | 0.9030 | 567.8 | 0.9808 | 573.6 | 0.9941 |
| 562.2 | 0.8972 | 568 | 0.9743 | 573.8 | 0.9814 |
| 562.4 | 0.9003 | 568.2 | 0.9738 | 574 | 0.9860 |
| 562.6 | 0.9006 | 568.4 | 0.9736 | 574.2 | 0.9879 |
| 562.8 | 0.9085 | 568.6 | 0.9759 | 574.4 | 0.9999 |
| 563 | 0.9046 | 568.8 | 0.9821 | 574.6 | 0.9973 |
| 563.2 | 0.8960 | 569 | 0.9787 | 574.8 | 0.9988 |
| 563.4 | 0.8881 | 569.2 | 0.9860 | 575 | 1.0016 |
| 563.6 | 0.9059 | 569.4 | 0.9755 | 575.2 | 1.0139 |
| 563.8 | 0.9178 | 569.6 | 0.9760 | 575.4 | 1.0186 |
| 564 | 0.9216 | 569.8 | 0.9809 | 575.6 | 1.0173 |
| 564.2 | 0.9224 | 570 | 0.9793 | 575.8 | 1.0156 |
| 564.4 | 0.9199 | 570.2 | 0.9859 | 576 | 1.0121 |
| 564.6 | 0.9254 | 570.4 | 0.9743 | 576.2 | 1.0257 |
| 564.8 | 0.9271 | 570.6 | 0.9740 | 576.4 | 1.0235 |
| 565 | 0.9366 | 570.8 | 0.9784 | 576.6 | 1.0263 |
| 565.2 | 0.9438 | 571 | 0.9806 | 576.8 | 1.0194 |
| 565.4 | 0.9314 | 571.2 | 0.9849 | 577 | 1.0115 |
| 565.6 | 0.9385 | 571.4 | 0.9716 | 577.2 | 1.0198 |
| 565.8 | 0.9444 | 571.6 | 0.9705 | 577.4 | 1.0204 |
| 566 | 0.9556 | 571.8 | 0.9756 | 577.6 | 1.0235 |
| 566.2 | 0.9609 | 572 | 0.9796 | 577.8 | 1.0127 |
| 566.4 | 0.9520 | 572.2 | 0.9888 | 578 | 1.0132 |
| 566.6 | 0.9496 | 572.4 | 0.9856 | 578.2 | 1.0219 |
| 566.8 | 0.9683 | 572.6 | 0.9869 | 578.4 | 1.0271 |
| 567 | 0.9649 | 572.8 | 0.9738 | 578.6 | 1.0429 |
| 567.2 | 0.9665 | 573 | 0.9848 | 578.8 | 1.0393 |
| 567.4 | 0.9656 | 573.2 | 0.9927 | 579 | 1.0378 |
| 567.6 | 0.9640 | 573.4 | 0.9920 | | |

| | | | | | |
|---|---|---|---|---|---|
| 579.2 | 1.0422 | 585 | 1.1330 | 590.8 | 1.0609 |
| 579.4 | 1.0476 | 585.2 | 1.1361 | 591 | 1.0720 |
| 579.6 | 1.0609 | 585.4 | 1.1214 | 591.2 | 1.0703 |
| 579.8 | 1.0612 | 585.6 | 1.1437 | 591.4 | 1.0400 |
| 580 | 1.0573 | 585.8 | 1.1457 | 591.6 | 1.0402 |
| 580.2 | 1.0503 | 586 | 1.1542 | 591.8 | 1.0467 |
| 580.4 | 1.0586 | 586.2 | 1.1429 | 592 | 1.0593 |
| 580.6 | 1.0656 | 586.4 | 1.1426 | 592.2 | 1.0460 |
| 580.8 | 1.0693 | 586.6 | 1.1625 | 592.4 | 1.0325 |
| 581 | 1.0696 | 586.8 | 1.1516 | 592.6 | 1.0288 |
| 581.2 | 1.0621 | 587 | 1.1698 | 592.8 | 1.0049 |
| 581.4 | 1.0706 | 587.2 | 1.1481 | 593 | 1.0234 |
| 581.6 | 1.0733 | 587.4 | 1.1397 | 593.2 | 1.0152 |
| 581.8 | 1.0826 | 587.6 | 1.1436 | 593.4 | 0.9871 |
| 582 | 1.0828 | 587.8 | 1.1478 | 593.6 | 0.9720 |
| 582.2 | 1.0692 | 588 | 1.1652 | 593.8 | 0.9694 |
| 582.4 | 1.0790 | 588.2 | 1.1446 | 594 | 0.9805 |
| 582.6 | 1.0804 | 588.4 | 1.1405 | 594.2 | 0.9703 |
| 582.8 | 1.1072 | 588.6 | 1.1320 | 594.4 | 0.9642 |
| 583 | 1.0985 | 588.8 | 1.1346 | 594.6 | 0.9421 |
| 583.2 | 1.1040 | 589 | 1.1424 | 594.8 | 0.9317 |
| 583.4 | 1.1019 | 589.2 | 1.1273 | 595 | 0.9324 |
| 583.6 | 1.1337 | 589.4 | 1.1182 | 595.2 | 0.9372 |
| 583.8 | 1.1397 | 589.6 | 1.0906 | 595.4 | 0.9369 |
| 584 | 1.1337 | 589.8 | 1.0960 | 595.6 | 0.8959 |
| 584.2 | 1.1356 | 590 | 1.0994 | 595.8 | 0.8900 |
| 584.4 | 1.1278 | 590.2 | 1.0814 | 596 | 0.8892 |
| 584.6 | 1.1428 | 590.4 | 1.0778 | 596.2 | 0.8859 |
| 584.8 | 1.1288 | 590.6 | 1.0507 | | |

| | | | | | |
|---|---|---|---|---|---|
| 596.4 | 0.8933 | 602.2 | 0.7705 | 608 | 0.4208 |
| 596.6 | 0.8811 | 602.4 | 0.7956 | 608.2 | 0.3985 |
| 596.8 | 0.8614 | 602.6 | 0.7829 | 608.4 | 0.3905 |
| 597 | 0.8452 | 602.8 | 0.7749 | 608.6 | 0.3878 |
| 597.2 | 0.8602 | 603 | 0.7384 | 608.8 | 0.3947 |
| 597.4 | 0.8780 | 603.2 | 0.7236 | 609 | 0.3851 |
| 597.6 | 0.8657 | 603.4 | 0.7146 | 609.2 | 0.3602 |
| 597.8 | 0.8709 | 603.6 | 0.6850 | 609.4 | 0.3530 |
| 598 | 0.8655 | 603.8 | 0.6811 | 609.6 | 0.3328 |
| 598.2 | 0.8779 | 604 | 0.6340 | 609.8 | 0.3407 |
| 598.4 | 0.8830 | 604.2 | 0.6169 | 610 | 0.3191 |
| 598.6 | 0.8910 | 604.4 | 0.6085 | 610.2 | 0.3081 |
| 598.8 | 0.8965 | 604.6 | 0.5955 | 610.4 | 0.2803 |
| 599 | 0.8814 | 604.8 | 0.6039 | 610.6 | 0.2674 |
| 599.2 | 0.8800 | 605 | 0.5607 | 610.8 | 0.2710 |
| 599.4 | 0.8888 | 605.2 | 0.5456 | 611 | 0.2479 |
| 599.6 | 0.8810 | 605.4 | 0.5384 | 611.2 | 0.2318 |
| 599.8 | 0.8579 | 605.6 | 0.5388 | 611.4 | 0.2116 |
| 600 | 0.8548 | 605.8 | 0.5367 | 611.6 | 0.1997 |
| 600.2 | 0.8416 | 606 | 0.5157 | 611.8 | 0.1983 |
| 600.4 | 0.8693 | 606.2 | 0.5026 | 612 | 0.1892 |
| 600.6 | 0.8612 | 606.4 | 0.4712 | 612.2 | 0.1843 |
| 600.8 | 0.8434 | 606.6 | 0.4732 | 612.4 | 0.1600 |
| 601 | 0.8303 | 606.8 | 0.4766 | 612.6 | 0.1567 |
| 601.2 | 0.8122 | 607 | 0.4661 | 612.8 | 0.1510 |
| 601.4 | 0.8347 | 607.2 | 0.4401 | 613 | 0.1383 |
| 601.6 | 0.8132 | 607.4 | 0.4354 | 613.2 | 0.1412 |
| 601.8 | 0.8034 | 607.6 | 0.4281 | 613.4 | 0.1253 |
| 602 | 0.7898 | 607.8 | 0.4310 | | |

| | |
|---|---|
| 613.6 | 0.1107 |
| 613.8 | 0.0923 |
| 614 | 0.0872 |
| 614.2 | 0.0766 |
| 614.4 | 0.0723 |
| 614.6 | 0.0655 |
| 614.8 | 0.0579 |
| 615 | 0.0494 |
| 615.2 | 0.0401 |
| 615.4 | 0.0424 |
| 615.6 | 0.0262 |
| 615.8 | 0.0166 |
| 616 | 0.0146 |

# Acknowledgement

First and foremost, I would like to extend my greatest thanks to Prof. Akira Harata. During these several years of studying in Kyushu University, Prof. Akira Harata cares so much about not only my study but also my life. Prof. Akira Harata often discusses academic questions with me, revises papers for me, and even introduces jobs for me. I will be keeping grateful for the great help from Prof. Akira Harata.

I would also like to give my earnest thanks to Assistant Prof. Toshio Ishioka for his instructions, advices and encouragement. Moreover, I am also very thankful for kind help and deep discussions from Prof. Kenji Furuya, Associate Prof. Akihiro Yabushita, and Ms. Miki Isoda, and for good comments from Prof. Seigi Mizuno and Prof. Hirotsugu Kikuchi.

Thanks are also extended to all students in our laboratory who helped me in life and study during these years. Among them, I would like to give my special thanks to Mr. Yasushi Imanishi for his help in starting my research topic and his contribution in my research work, and to Mr. Shoichiro Furukawa, Mr. Satoshi Yoshikawa, Mr. Toshio Morimoto and Mr. Takayasu Asou for their substantial help in my life when I first came to Japan.

I also want to express my great gratitude to Ministry of Education, Culture, Sports, Science and Technology, the Government of Japan, for providing me the Japanese Government Scholarship for three years.

I also sincerely appreciate Prof. Jinfang Zhi for her kind recommending me as one student of Prof. Akira Harata to have such a rare chance to study in Kyushu University for a doctorate under financial support of the Japanese Government Scholarship.

Finally, I would like to thank all of my relatives and friends in China, for their consistent understanding, supporting and encouragement.